

How the Magondi Belt lost its length:

Chemostratigraphic test for correlation in Central African
Precambrian metamorphic belts

Sharad Master¹ and Andrey Bekker²

¹EGRI, School of Geosciences, University of the
Witwatersrand, Johannesburg, South Africa,
sharad.master@wits.ac.za

²Dep. of Earth Sciences, University of California
Riverside, Riverside, California, USA

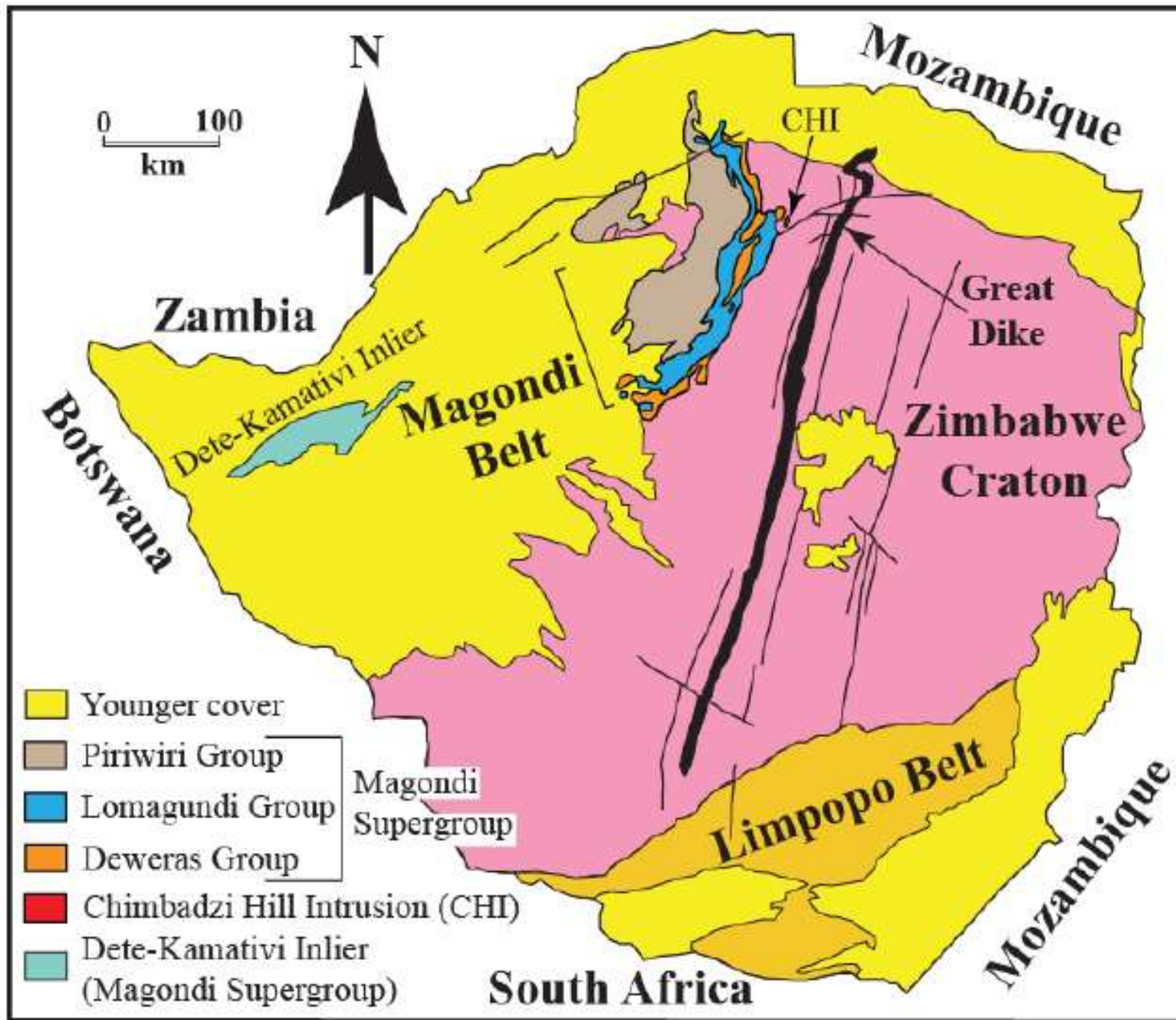
With apologies to Rudyard Kipling's Just So Stories

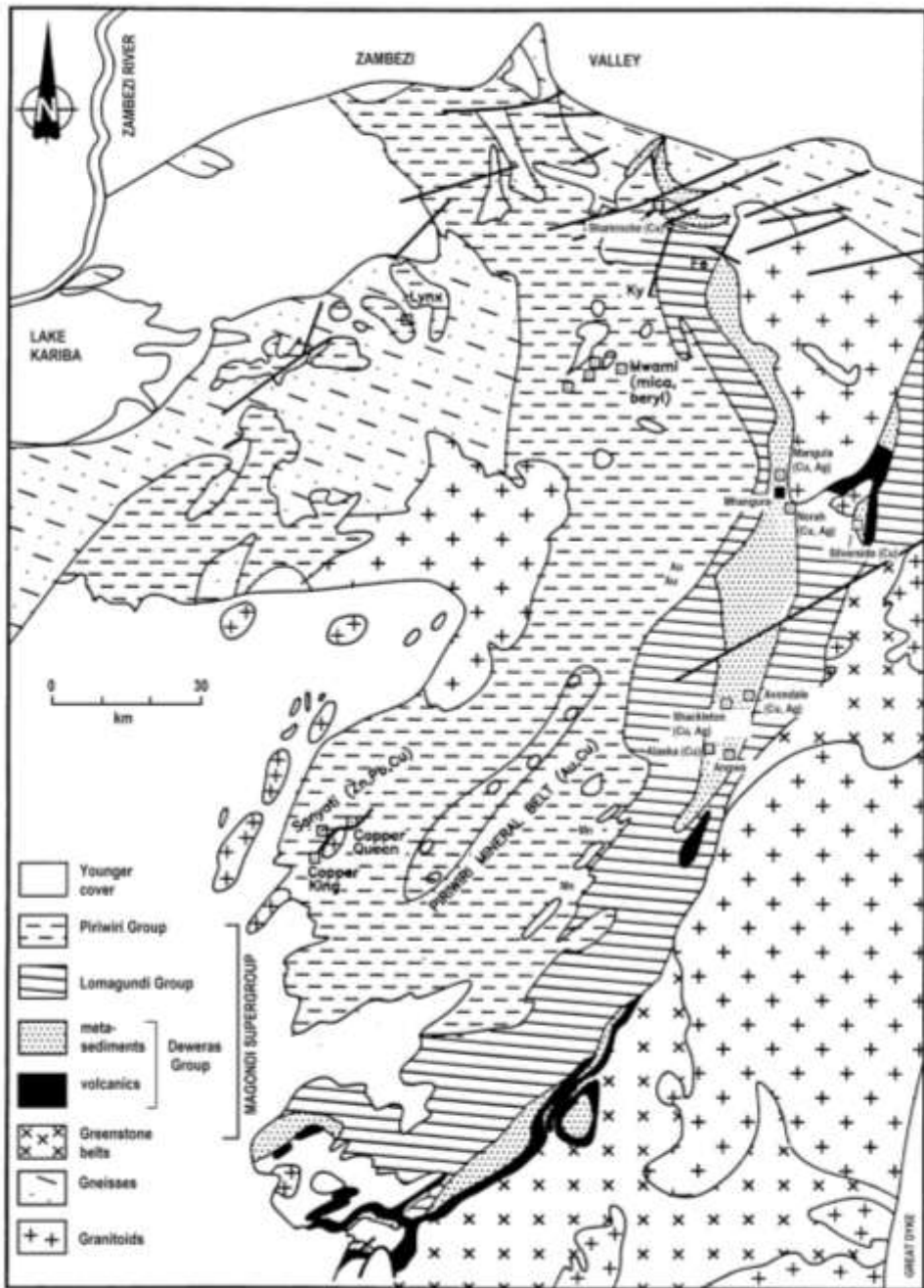
How the Elephant got his trunk



Part 1. How the Magondi Belt got its length

The Palaeoproterozoic Magondi Supergroup, Zimbabwe





- Generalised stratigraphy, lithology and environments of the Magondi Supergroup.

Group	Lithology	Environment
-------	-----------	-------------

Piriwiri	graphitic schists, wackes, cherts, siltites, phyllites, greywackes, agglomerates, andesitic to felsic lavas, tuffs and agglomerates, dolomites, massive sulphides, Mn beds	Deep marine, distal shelf, continental slope, submarine fan
-----------------	--	---

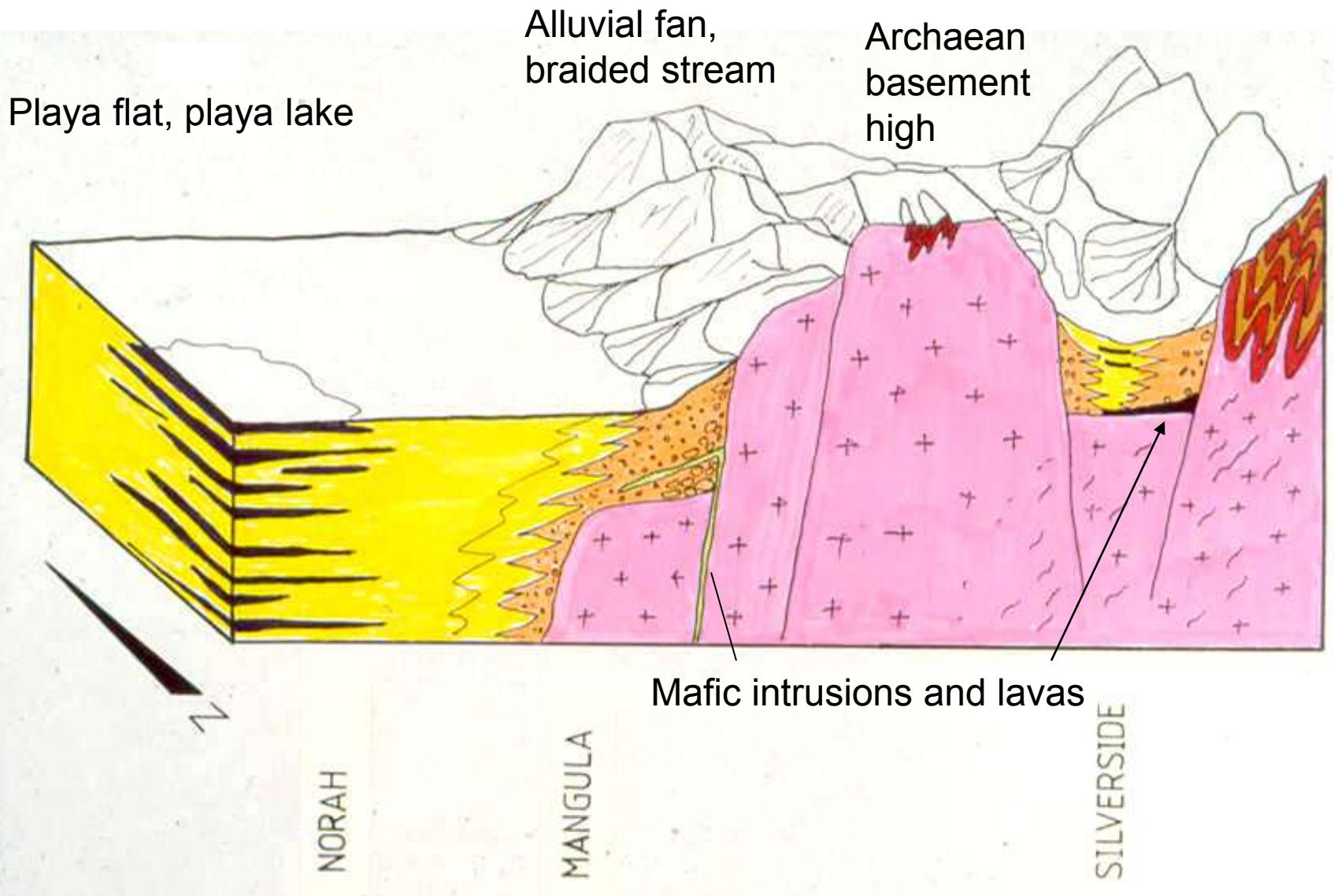
Lomagundi	conglomerates, arkosic arenites, orthoquartzites, stromatolitic dolomites, banded iron-formation, striped and graphitic slates, felsites, agglomerates, wackes.	Marginal marine (peritidal) and shallow storm-dominated shelf
------------------	---	---

----- unconformity -----

Deweras	conglomerates, arkosic arenites, siltites, argillites, dolomites, evaporates, basaltic lavas and pyroclastics, flats, aeolian	Continental alluvial fans, braided streams, playa dunes, playa lakes
----------------	---	--

----- unconformity -----

Basement Complex (Archaean granite-greenstone terrain of Zimbabwe Craton)



Palaeoenvironments, Deweras Group



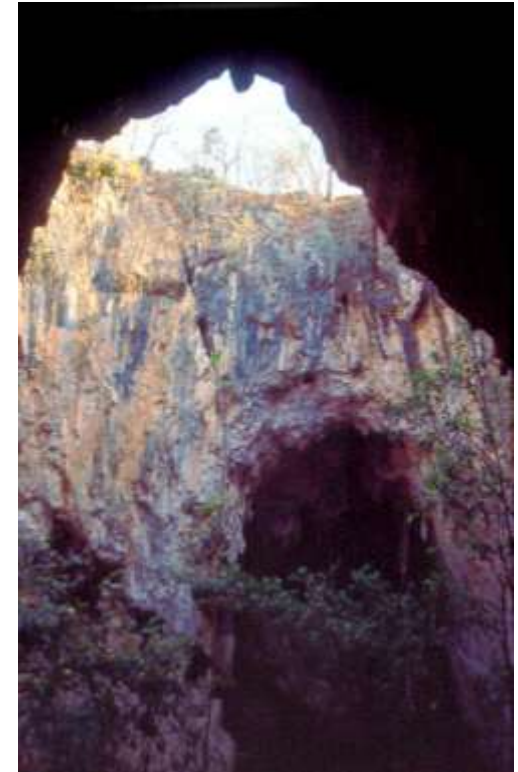
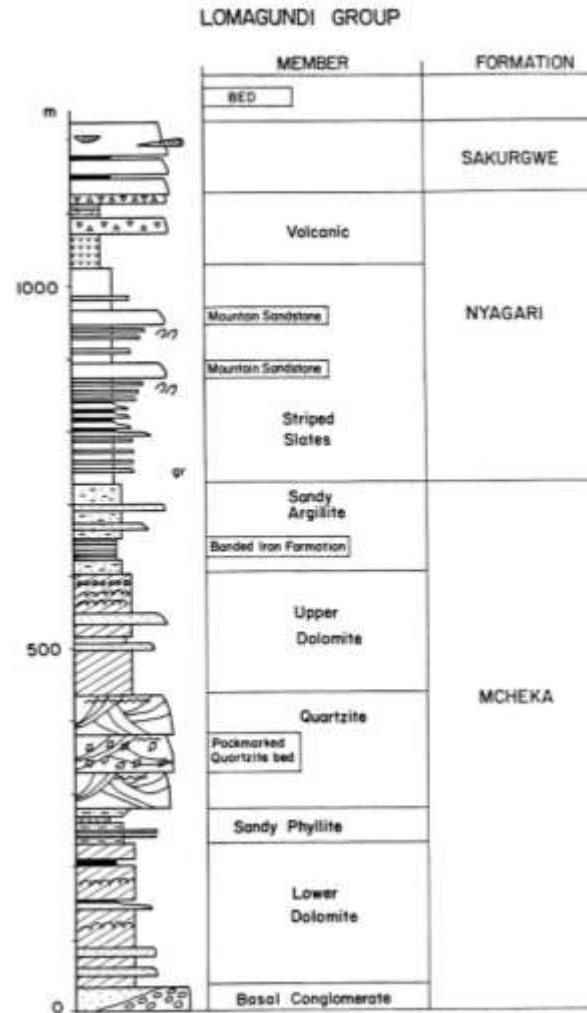
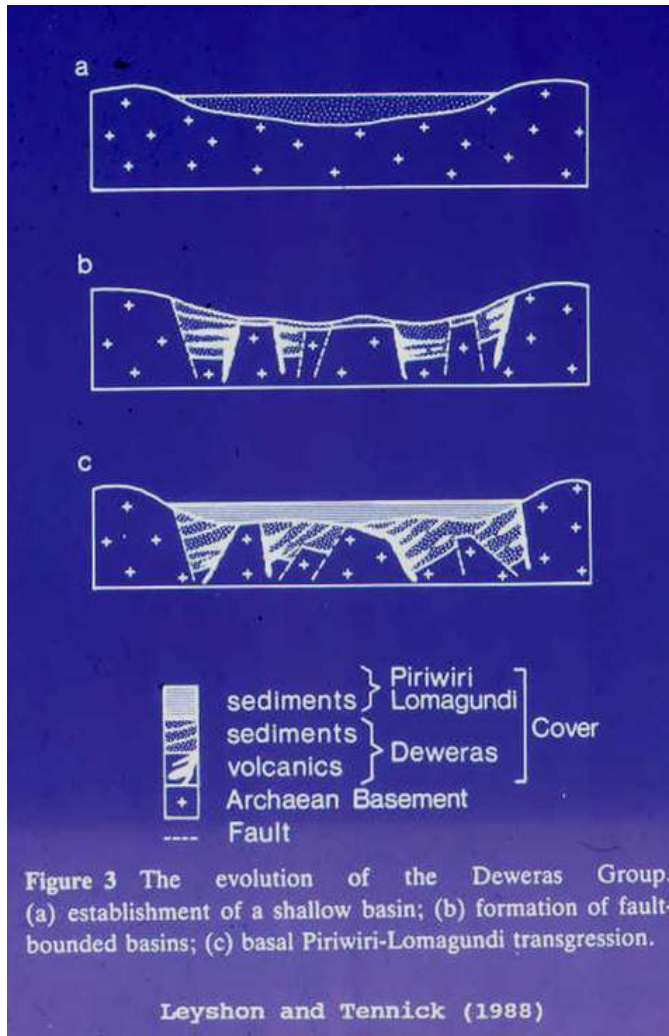
Arkoses in Deweras Group with abundant detrital magnetites on trough-crossbed foresets (fluvial environment).



Anhydrite-bearing dolomites, Deweras Group

Master et al., 2010, Precambrian Research

Lomagundi Group- post-rift sag basin carbonate platform





Lower Dolomite, Mcheka Formation, Lomagundi Group



Lower Dolomite, Mcheka Formation, Lomagundi Group

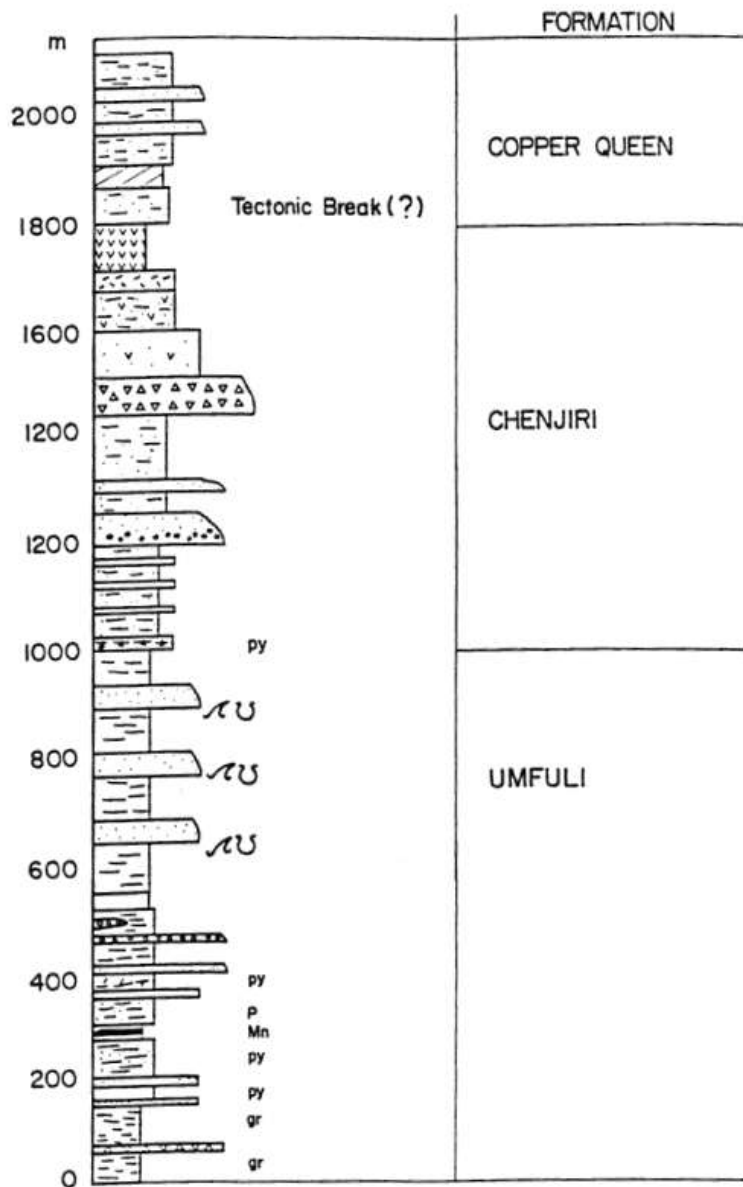


Upper Dolomite, Mcheka Formation, Lomagundi Group

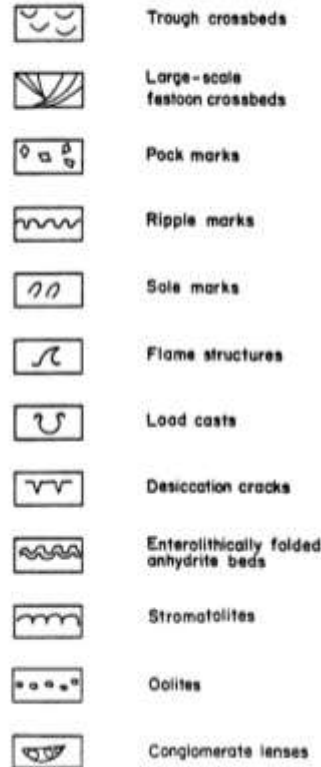
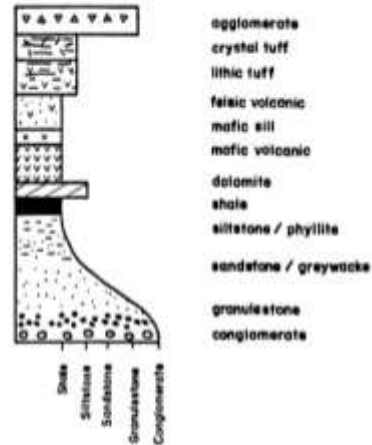


Plan view of deformed domical stromatolites, Lower Dolomite,
Lomagundi Group

PIRIWIRI GROUP



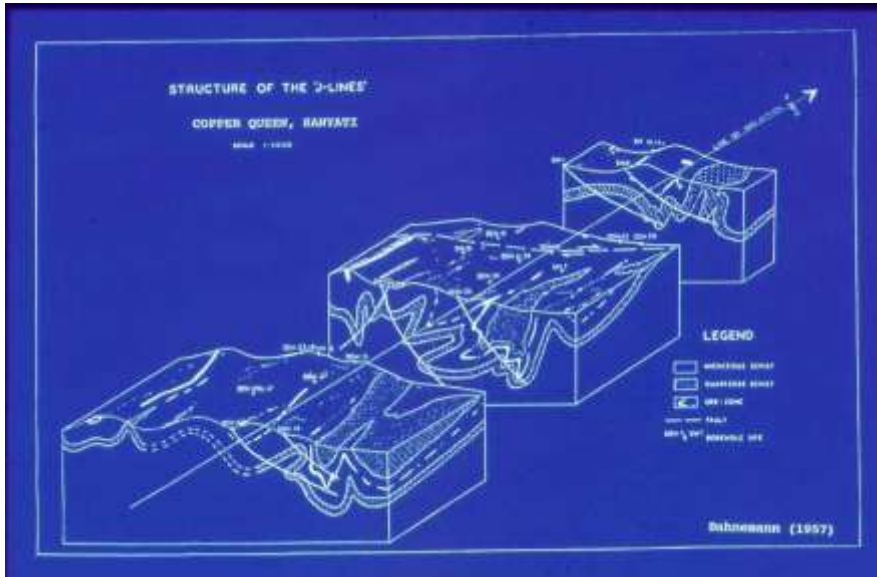
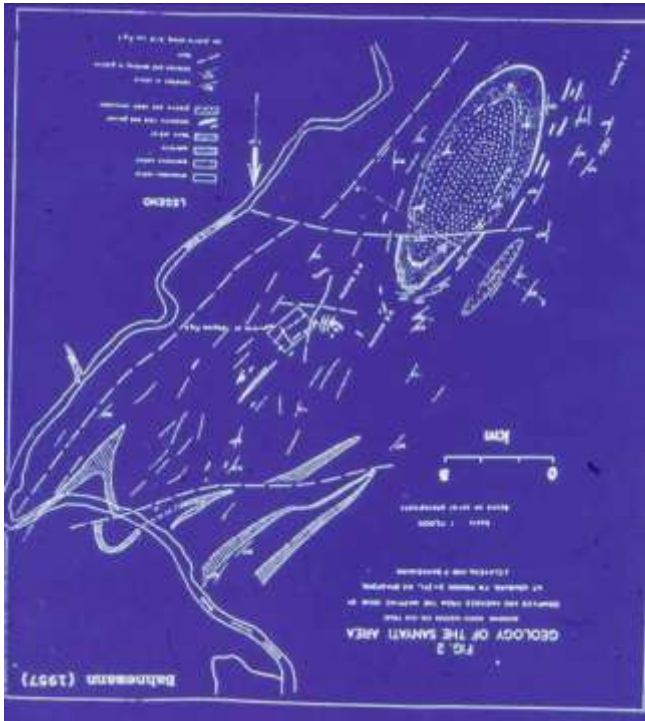
KEY

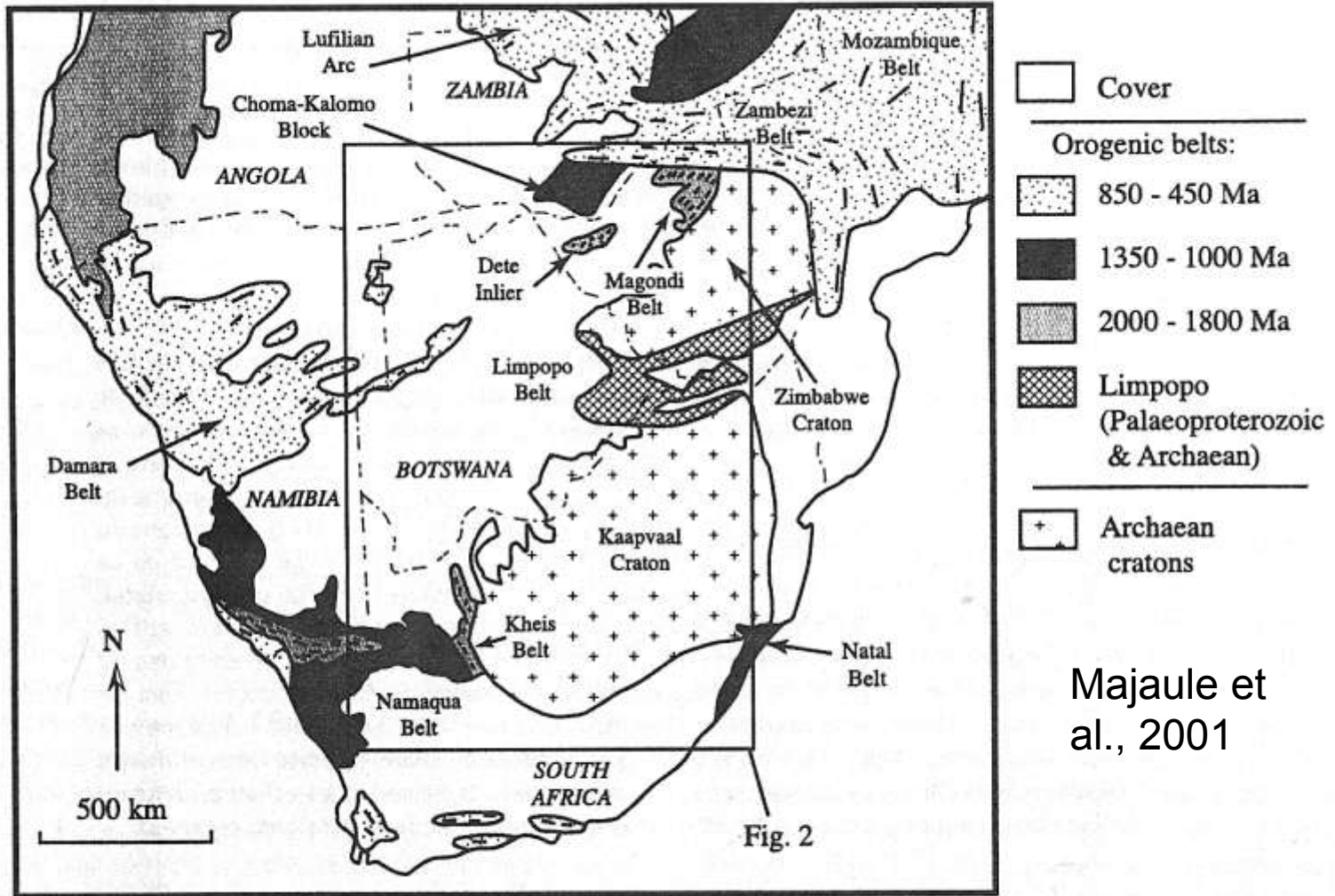


- cu copper sulphides
- py pyrite
- gr graphite
- mn manganese oxides
- p phosphate (collophanite)

Copper Queen Cu-Zn-(Pb)-(Ag) SHMS deposit, Piriwiri Group

Deeper water facies
equivalent of Lomagundi
Group. Massive sulphides
overlain by high $\delta^{13}\text{C}$
carbonates





Majaule et al., 2001

Figure 1. Simplified map of the Precambrian tectonic framework of southern Africa, showing exposed parts of Proterozoic orogenic belts and Archaean cratons. The Limpopo Belt includes both Archaean and Palaeoproterozoic components. Location of Fig. 2 is indicated.

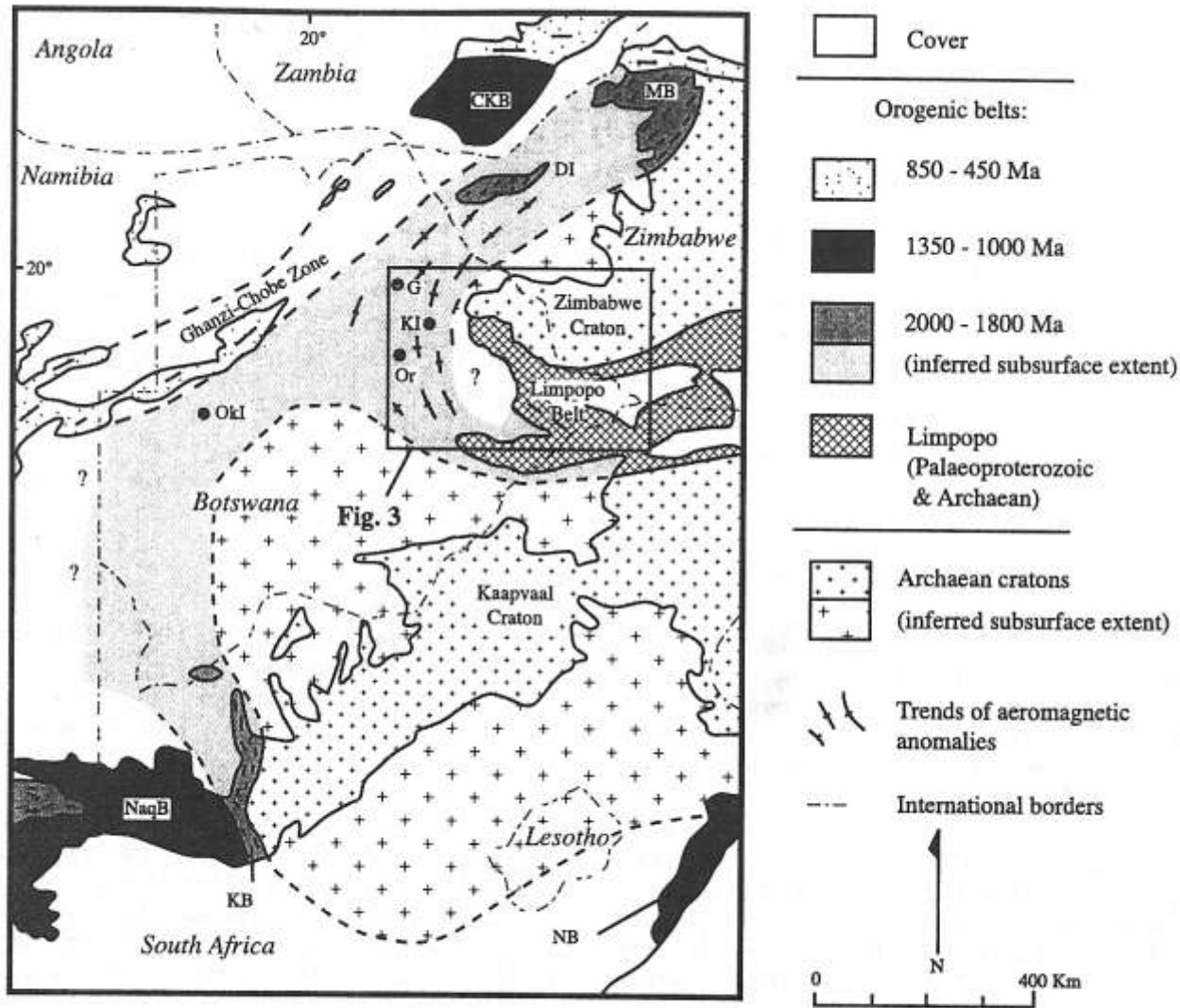


Figure 2. Regional Precambrian tectonic framework of Botswana and adjacent areas (modified primarily from Carney et al., 1994; Thomas et al., 1994). CKB: Choma-Kalomo Block; MB: Magondi Belt; DI: Dete Inlier; G: Gweta; KI: Kubu Island; Or: Orapa diamond mine; OkI: Okwa Inlier; NaqB: Namaqua Belt; KB: Kheis Belt; NB: Natal Belt. Location of Fig. 3 is indicated.

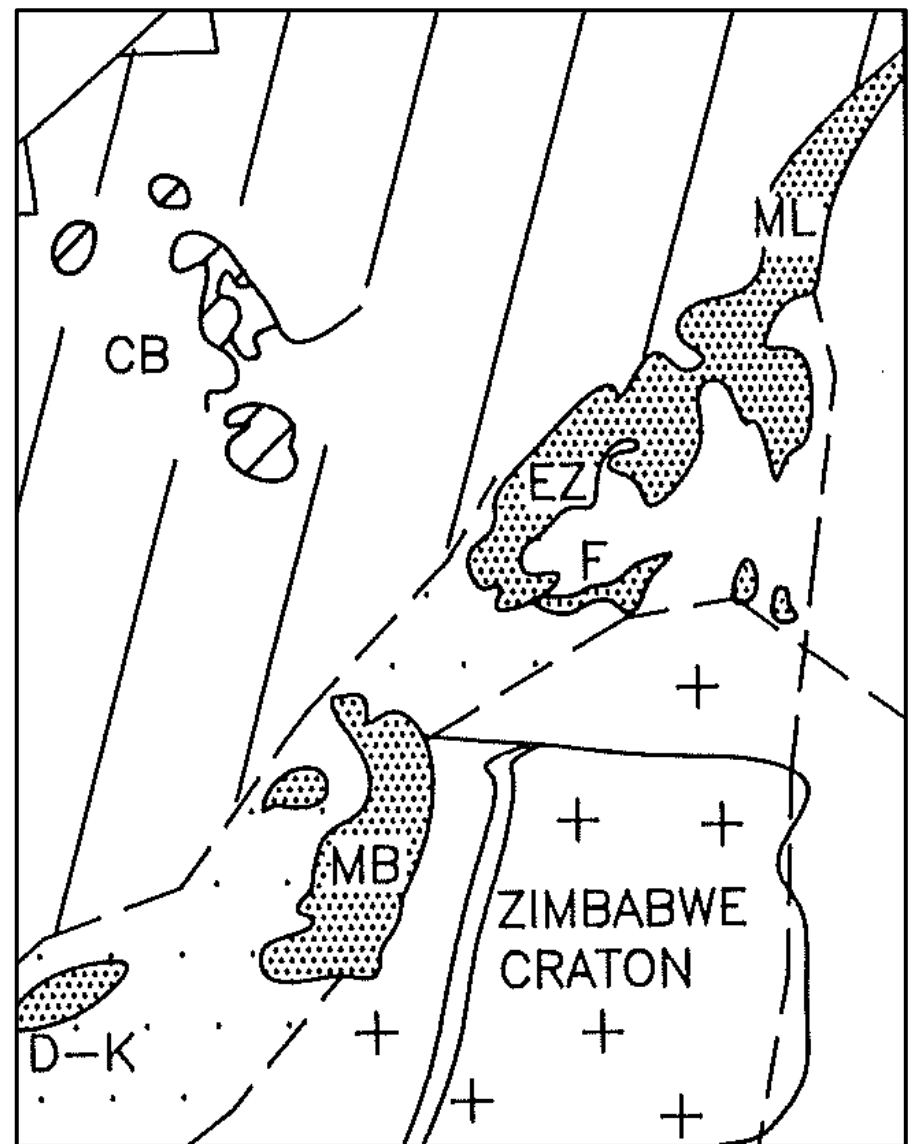
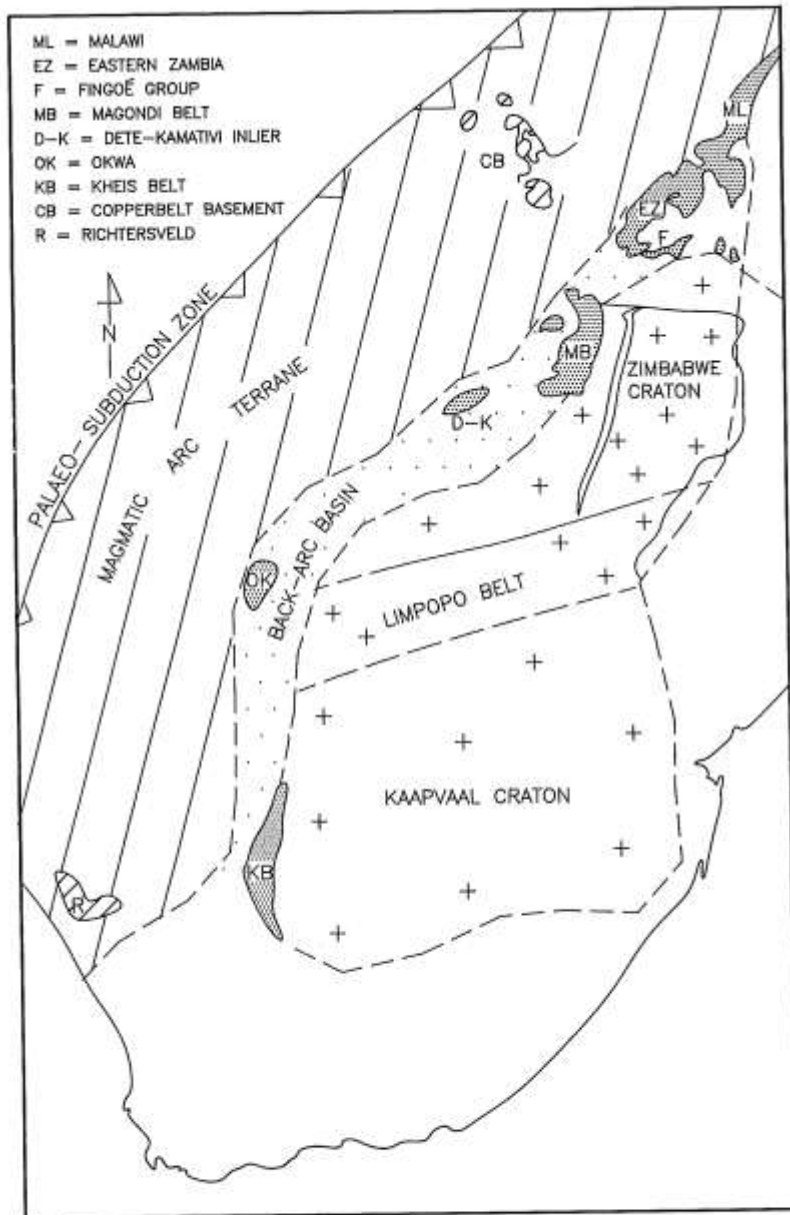
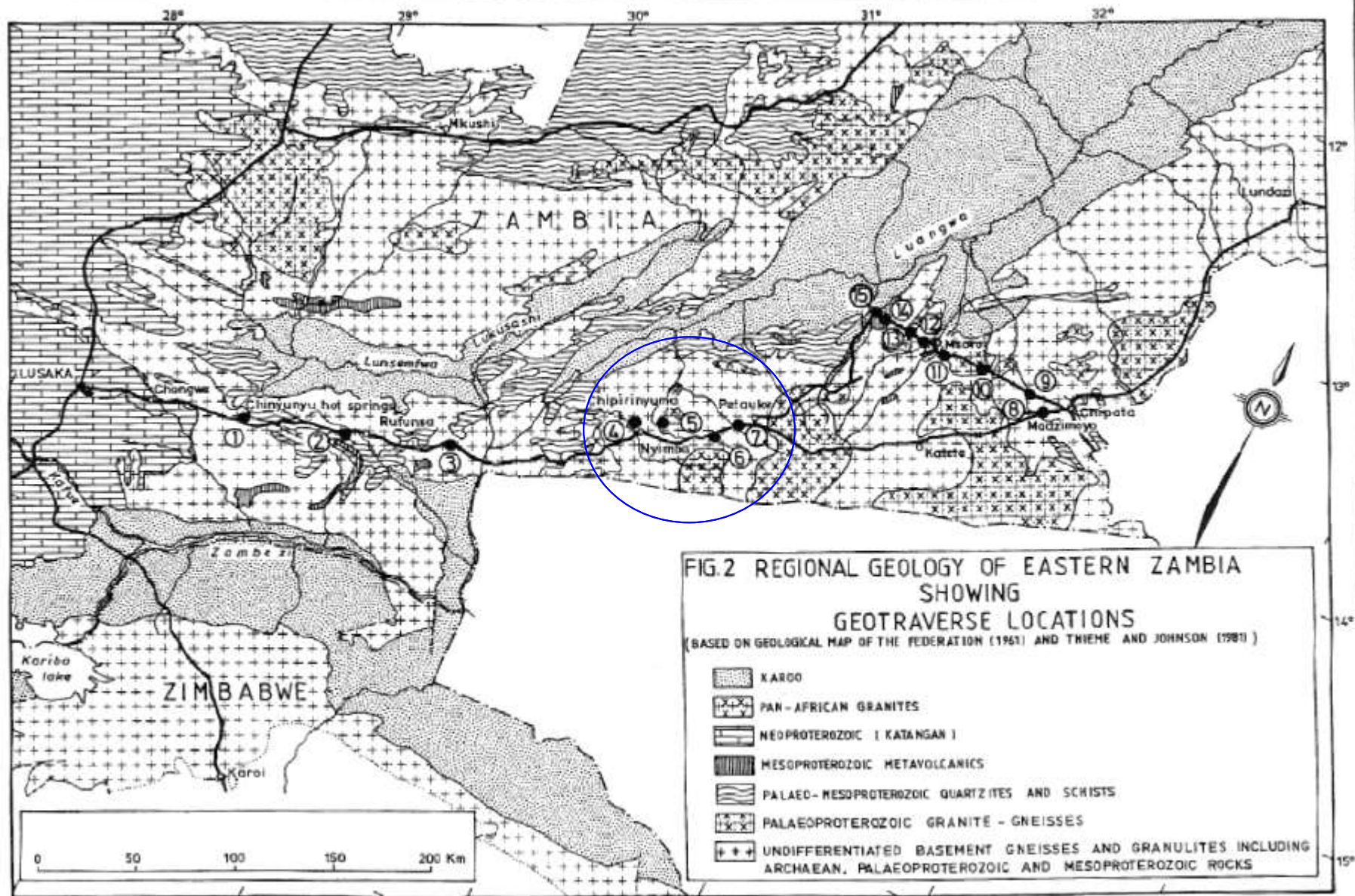


Figure 9: Schematic plan showing position of Magondi Supergroup and correlative sequences in a continental back-arc basin, with respect to the postulated magmatic arc terrane, palaeo-subduction zone, and the combined Zimbabwe-Limpopo-Kaapvaal continent (after Master, 1990d, 1991).

Master (1991a,b, 1994)



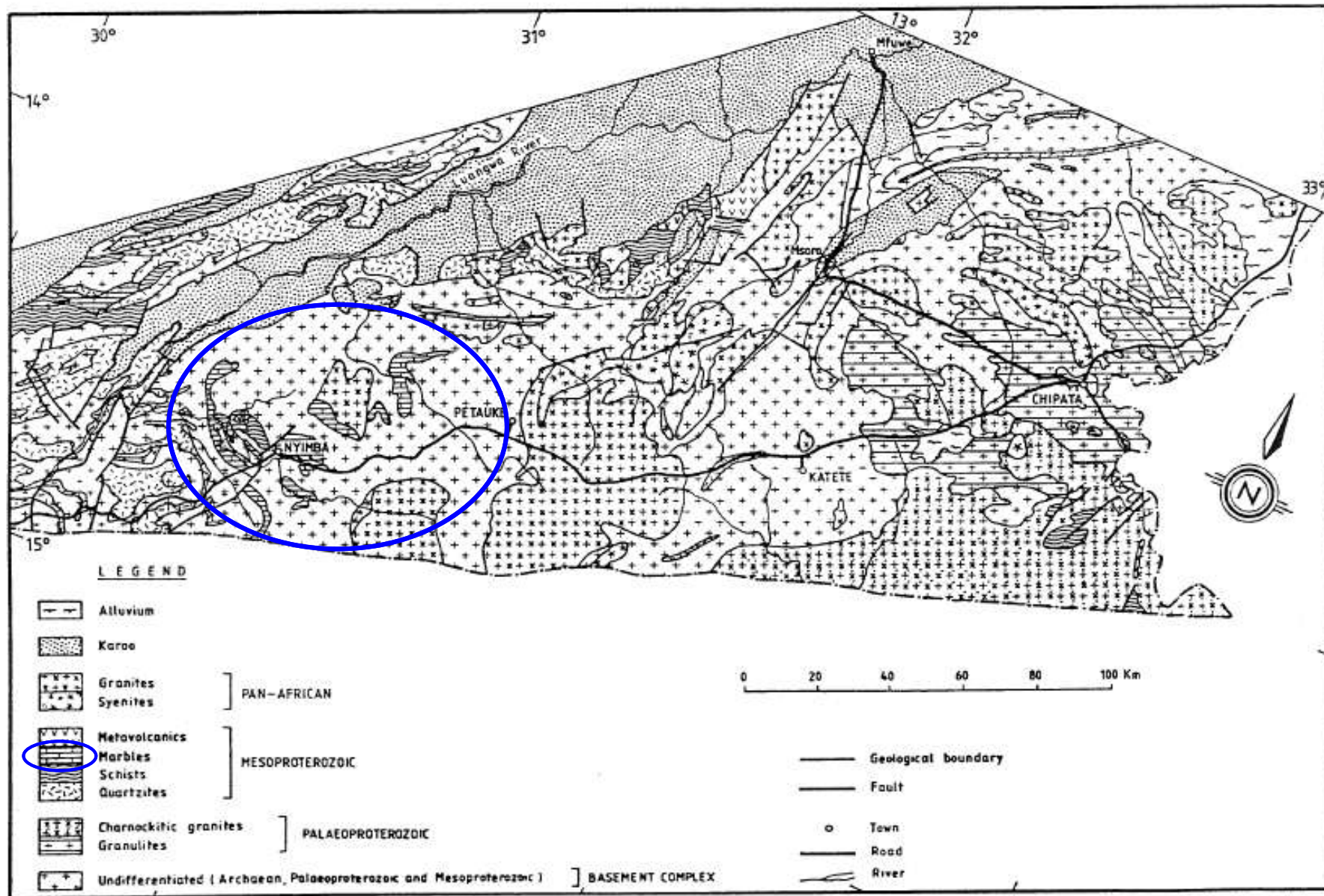


FIG. 3 GEOLOGICAL MAP OF NYIMBA — CHIPATA AREA (BASED ON THIEME AND JOHNSON, 1981)

Kamona, Tembo, Sikazwe, Siegfried, Master, 1996. IGCP 363 Excursion Guidebook

Northern continuation of Magondi Belt? (Master, 1991a,d; 1994)

Magondi Belt, NW Zimbabwe

- Deweras Group
 - Arkose, pelite, carbonates, mafic volcanics
- Lomagundi, Piriwiri Groups
 - quartzite, dolostones, black shales, graphitic schists, Cu-Pb-Zn massive sulphides
 - *Greenschist – amphibolite facies metamorphism*

Sinda, Lusandwa and Mvuvye terranes, Eastern Zambia

- Sinda, Lusandwa Groups
 - quartzo-feldspathic gneisses, schists, marbles, amphibolites
- Mvuvye Group
 - quartzite, marbles, graphite schists; Cu-Pb-Zn massive sulphides
 - *Amphibolite- granulite facies metamorphism*

- The Magondi basin developed from continental rift to passive margin (and later to a foreland basin), and in the marine successions there are represented both proximal shallow water and distal deep water facies, and in all facies there are ^{13}C -enriched carbonate rocks.

2. Carbon isotope anomalies and use of high $\delta^{13}\text{C}$ carbonate rocks in chemostratigraphic correlation

Precambrian Research, 2 (1975) 2 (1975) 1–69

© Elsevier Scientific Publishing Company, Amsterdam — Printed in The Netherlands

**PRECAMBRIAN SEDIMENTARY CARBONATES: CARBON AND OXYGEN
ISOTOPE GEOCHEMISTRY AND IMPLICATIONS FOR THE TERRESTRIAL
OXYGEN BUDGET***

MANFRED SCHIDLOWSKI, RUDOLF EICHMANN and CHRISTIAN E. JUNGE

Max-Planck-Institut für Chemie, Mainz (G.F.R.)

(Received March 20, 1974; accepted July 1, 1974)

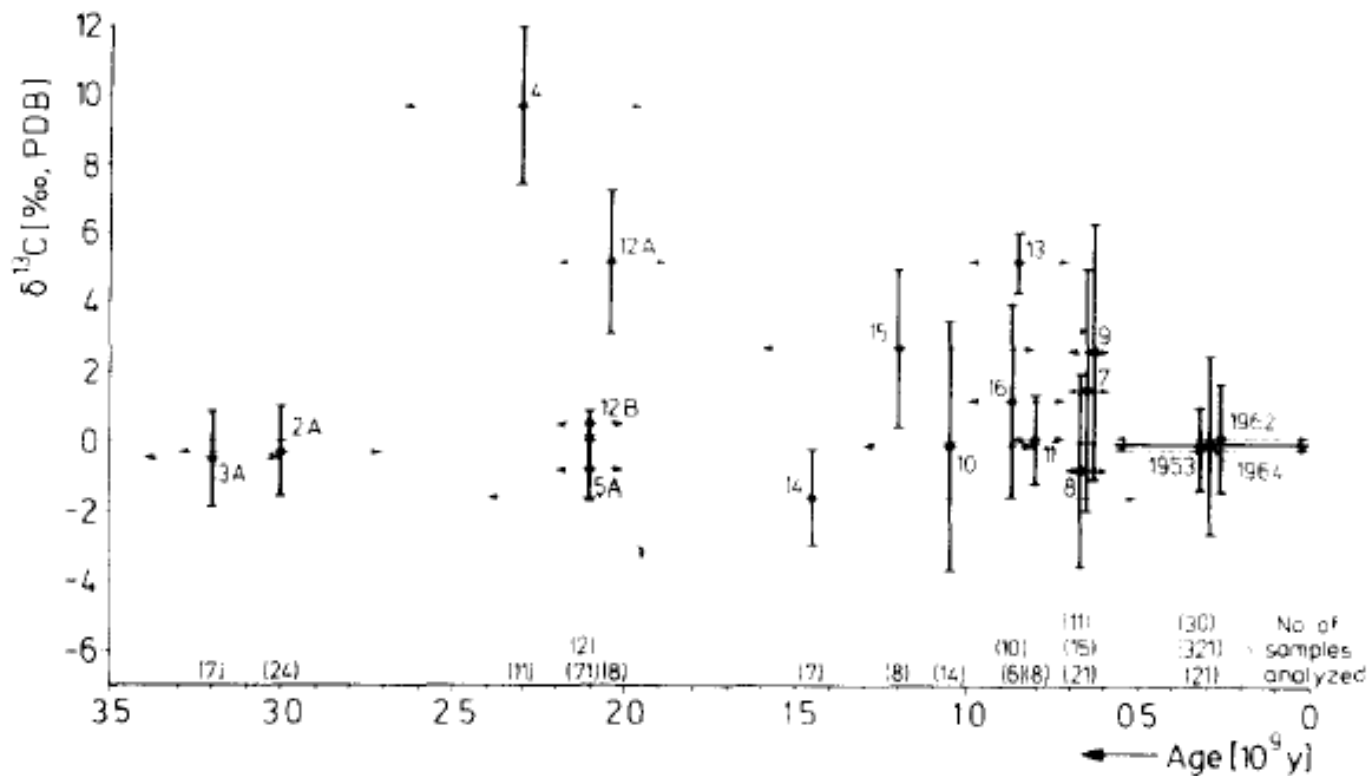


Fig.11. Carbon isotope composition of substantially unaltered sedimentary carbonates as a function of geologic time. Mean $\delta^{13}\text{C}$ values of carbonate groups investigated are indicated by circles, the vertical bars representing the standard deviation; horizontal arrows show possible geological time range. Numbers refer to Tables IIA—XVI listing the values yielded by individual samples of each group or locality. (Values for Phanerozoic carbonates ($< 0.57 \cdot 10^9\text{y}$) according to Craig, 1953; Degens and Epstein, 1962; Keith and Weber, 1964.)

Schidlowski, Eichmann & Junge, 1975

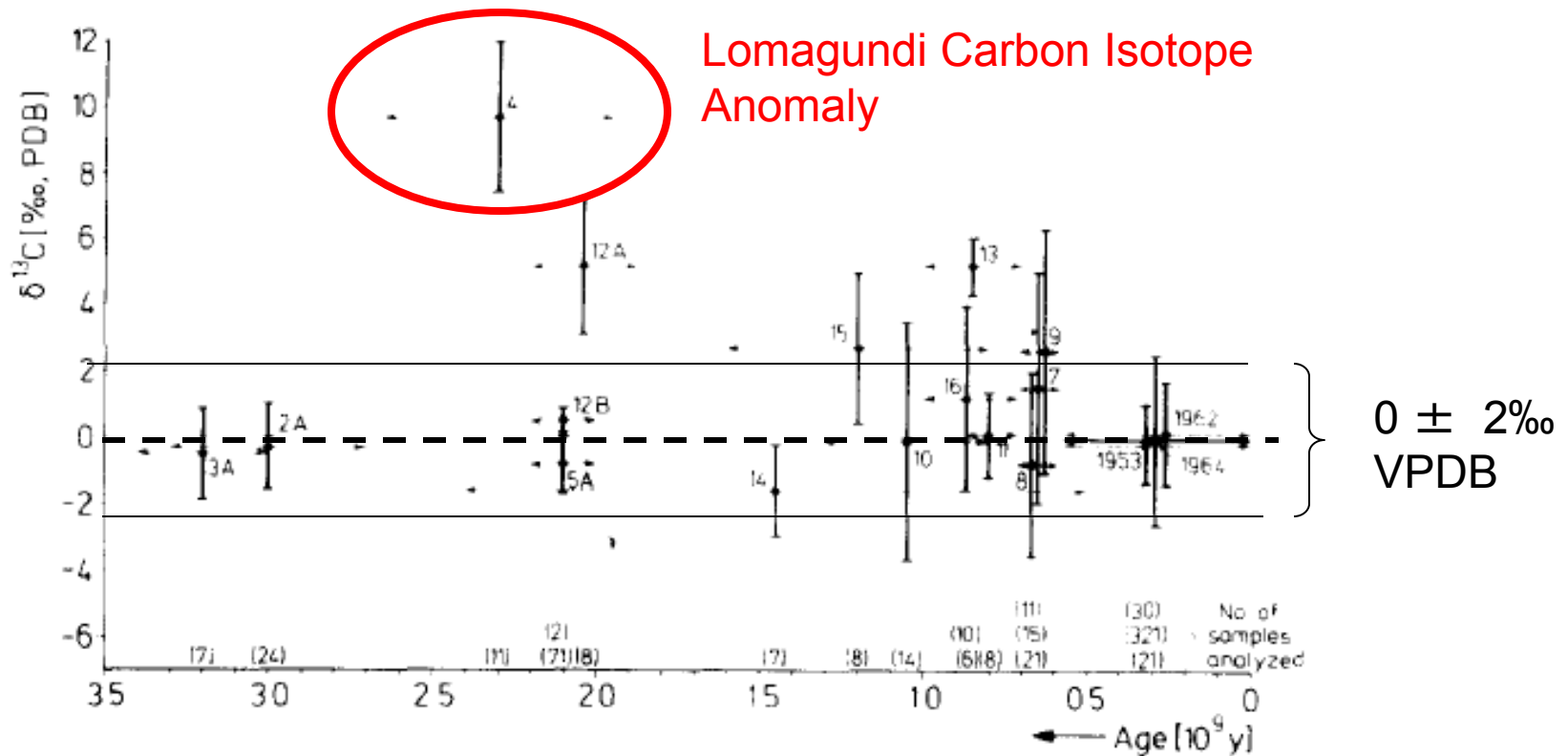


Fig.11. Carbon isotope composition of substantially unaltered sedimentary carbonates as a function of geologic time. Mean $\delta^{13}\text{C}$ values of carbonate groups investigated are indicated by circles, the vertical bars representing the standard deviation; horizontal arrows show possible geological time range. Numbers refer to Tables IIA—XVI listing the values yielded by individual samples of each group or locality. (Values for Phanerozoic carbonates ($< 0.57 \cdot 10^9\text{y}$) according to Craig, 1953; Degens and Epstein, 1962; Keith and Weber, 1964.)

Schidlowski, Eichmann & Junge, 1975

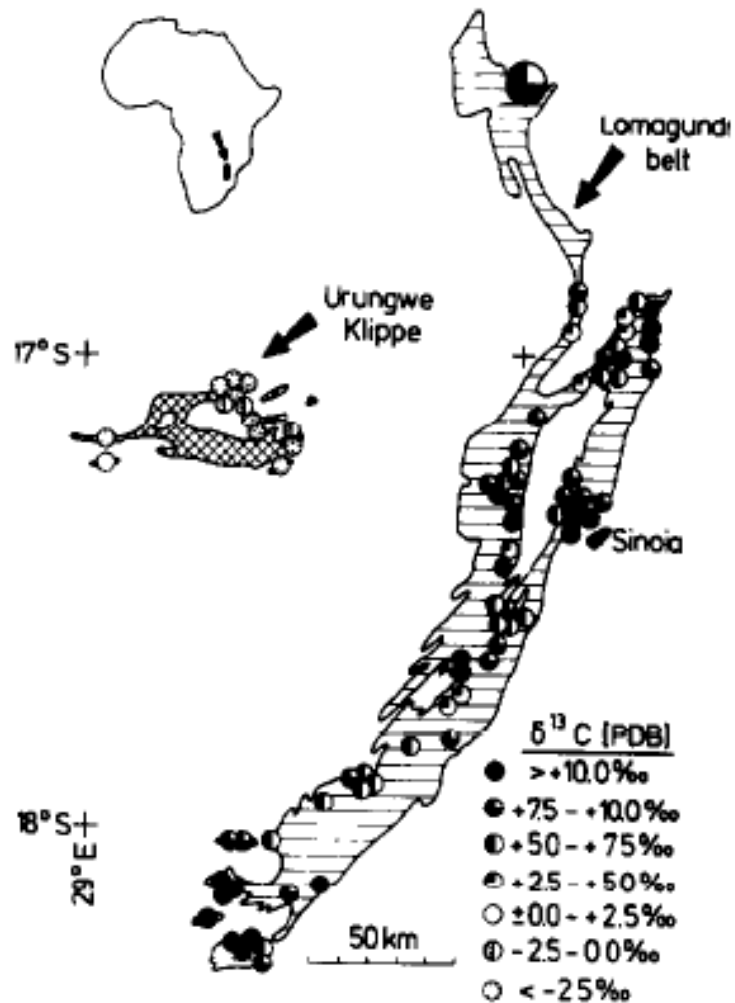


Fig. 2. Outcrops of Lomagundi sediments (hatched, Lomagundi belt) or rocks of assumed Lomagundi association (crosshatched, Urungwe klippe) with regional distribution pattern of $\delta^{13}\text{C}$ values yielded by the intercalated carbonates. Major circle near northern tip of Lomagundi belt shows average for Shamrocke Mine area (R. H. Thole, personal communication, 1974). For situation of the area cf. key map in upper left corner.

Schidlowski,
Eichmann &
Junge, 1976

In a reconnaissance isotopic study of global Precambrian carbonates, by Schidlowski et al. (1975), the carbonate rocks of the Lomagundi Group were found to be the most isotopically anomalous regional carbonate province in the world, being **very enriched in ^{13}C** , with an average $\delta^{13}\text{C}$ value of +8.2‰ VPDB.

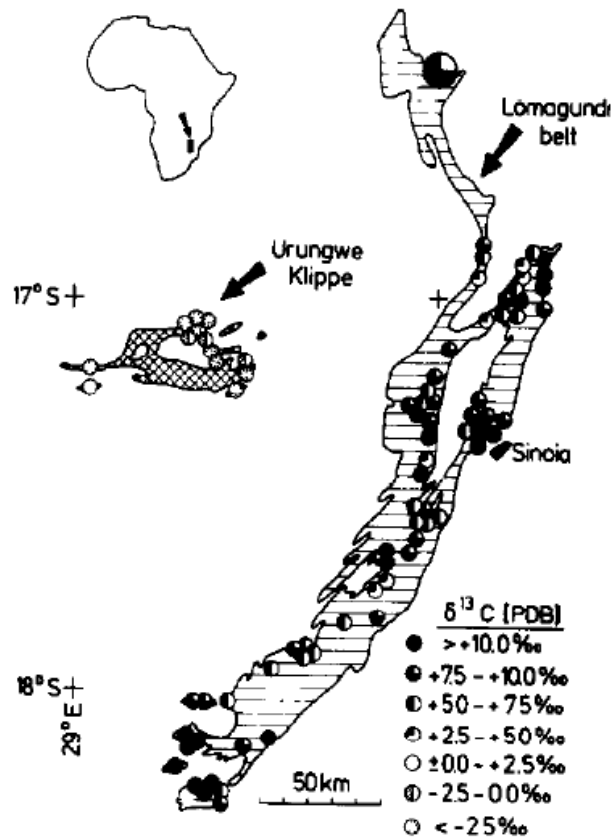
Subsequent work in the Magondi Basin has shown that high $\delta^{13}\text{C}$ carbonates are also present in the continental rocks of the underlying Deweras Group.

This isotopic anomaly has now been recognized globally in carbonate rocks deposited in the time span 2.24-2.06 Ga.

It is known as the Lomagundi Carbon Isotope Excursion



Fig.3. Geological sketch map of Rhodesia showing the localities (encircled numbers) within the ancient 'schist belts' (dotted areas) from where the carbonate samples listed in Table II have been collected. Other sampling localities refer to carbonates from the Lomagundi and Umkondo Groups (see Table IV) and from the circumcratonic belts (Table VI).



Carbon isotope geochemistry of the Precambrian Lomagundi carbonate province, Rhodesia

MANFRED SCHIDLowski, RUDOLF EICHMANN and CHRISTIAN E. JUNGE
Max-Planck-Institut für Chemie, D-6900 Mainz, Saarstr. 23, West Germany

(Received 18 March 1975; accepted in revised form 14 October 1975)

Abstract—Carbon isotope measurements carried out on 67 dolomite samples from the Middle Precambrian Lomagundi Group (Rhodesia) have yielded a $\delta^{13}\text{C}$ mean of $+8.2 \pm 2.6\text{‰}$ vs PDB. With the outcrop of these dolomites extending over a distance of almost 300 km, the Lomagundi dolomite facies is likely to represent the largest isotopically anomalous sedimentary carbonate province ever recorded. It is concluded that the anomalous carbonates formed in a closed basin whose $\delta^{13}\text{C}$ level had been substantially increased as a result of a preferential removal (within sedimentary organics) of the light carbon isotope.

Schidlowski et al. 1976

Fig. 2. Outcrops of Lomagundi sediments (hatched, Lomagundi belt) or rocks of assumed Lomagundi association (crosshatched, Urungwe klippe) with regional distribution pattern of $\delta^{13}\text{C}$ values yielded by the intercalated carbonates. Major circle near northern tip of Lomagundi belt shows average for Shamrocke Mine area (R. H. Thole, personal communication, 1974). For situation of the area cf. key map in upper left corner.

TABLE 1. CARBON ISOTOPE COMPOSITIONS OF CARBONATE AND SEDIMENTARY ORGANIC MATTER

Stratigraphic unit*	$\delta^{13}\text{C}_{\text{carb}}$ (‰, PDB)	<i>n</i>	$\delta^{13}\text{C}_{\text{org}}$ (‰, PDB)	<i>n</i>	Age (Ga)	Source of data†	Reference to age†
1. Wittenoom/Carawine Dolomite	-0.3 ± 1.5	103	-27.5 ± 9.2	17	2.603 ± 0.007	22, 25	8, 24, 10
2. Malmani/Campbellrand Subgroup	-0.7 ± 0.8	186	-31.6 ± 7.2	64	2.55 ± 0.01	22, 26	2, 11
3. Mt Sylvia and Mt McRae formations	-12.9 ± 3.9	29	-32.0 ± 6.5	7	2.54 ± 0.07	22	8, 24
4. Madetkoski Formation	-1.7	1			2.53 ± 0.05	12	12
5. Brockman Iron Formation	-9.6 ± 1.7	51			2.47 ± 0.07	22	24
6. Asbesheuvels and Koegas subgroups			-26.0 ± 6.4	4	2.43 ± 0.03	22	24
7. Itabira Group	-0.9 ± 1.4	9	-23.2 ± 1.9	10	2.42 ± 0.02	22	1
8. Seidorecha Formation	-2.7 ± 0.8	3			2.423 ± 0.007	12	12
9. Huronian Supergroup	-1.3 ± 0.5	35	-28.4 ± 3.8	26	2.34 ± 0.12	22, 26	6, 13
10. Sericite Schist Formation, Kausamo	8.1 ± 0.1	2			2.25 ± 0.05	12	12
11. Sompujärvi Formation	7.3 ± 1.2	3			2.25 ± 0.04	12§	12
12. Misi dolomite	12.6 ± 0.4	5			2.23 ± 0.07	12	12
13. Pretoria Group	0.8 ± 0.6	3	-23.2 ± 3.4	3	2.22 ± 0.02	22	28
14. Hotazel Formation	-10.0 ± 2.1	3			2.22 ± 0.02	22	28
15. Lower Viistola Formation	10.0 ± 0.7	5			2.113 ± 0.004	12	12
16. Piracicaba Group			-23.8 ± 5.5	15	2.10 ± 0.04	22	14, 1
17. Jouttiapa Formation	8.4 ± 1.6	10			2.09 ± 0.07	12	12
18. Lomagundi Group	8.4 ± 2.7	79	-23.9 ± 0.3	2	2.07 ± 0.10	22	23
19. Francevillian Series	4.3 ± 1.6	4	-31.7 ± 7.7	40	2.07 ± 0.05	7	4
20. Upper Petonen Formation	2.0 ± 1.4	2			2.062 ± 0.002	12	12
21. Belcher and Nastapoka groups	-1.3 ± 0.9	5	-23.4 ± 2.8	8	1.99 ± 0.04	22	5
22. Earahedy Group	-0.7 ± 1.2	8	-22.1 ± 6.5	22	1.98 ± 0.03	22	20
23. Svecofennian group	0.8 ± 1.1	52			1.92 ± 0.03	12	12
24. Coronation Supergroup	0.6 ± 1.6	33	-20.5 ± 6.0	19	1.91 ± 0.02	22, 27	27
25. Great Slave Supergroup	0.8 ± 1.1	6	-27.3 ± 8.2	4	1.90 ± 0.03	22	3
26. Amisk Group			-26.4 ± 2.8	40	1.89 ± 0.01	22	21
27. Koolpin Formation			-30.8 ± 0.3	2	1.885 ± 0.002	22	16, 18
28. Grythytan Slate			-28.6 ± 1.5	3	1.88 ± 0.02	22	29
29. Spartan Group			-29.9 ± 0.6	3	1.86 ± 0.02	22	15
30. Upper Wyloo Group	0.2 ± 1.2	32	-23.1 ± 2.9	13	1.843 ± 0.002	22, 27	19
31. Whitewater Group			-30.5 ± 5.0	5	1.75 ± 0.10	22	13
32. Urquhart Shale			-24.2 ± 2.1	33	1.653 ± 0.007	22	17, 18
33. McArthur Group	-1.1 ± 0.8	120	-29.7 ± 2.8	44	1.640 ± 0.007	22, 27	17, 18
34. Paradise Creek Formation			-28.9 ± 0.3	4	1.640 ± 0.007	22	17, 18
35. Changcheng group			-30.1 ± 2.0	19	1.62 ± 0.01	22	9

Note: Isotope data represent average $\delta^{13}\text{C}$ values ±1 standard deviation; PDB-Peedee belemnite standard.

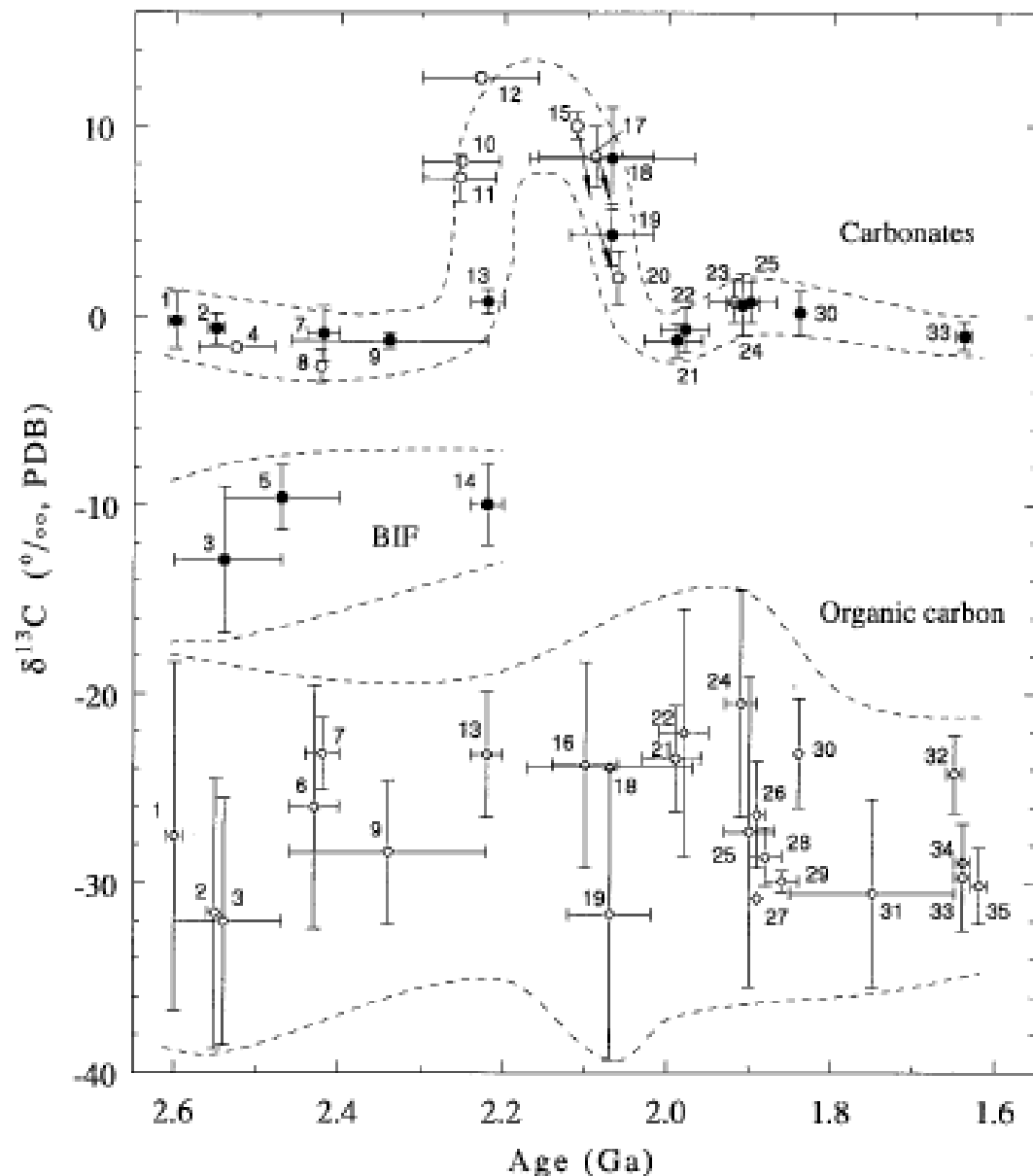
*Numbers refer to Figure 1 and to the text.

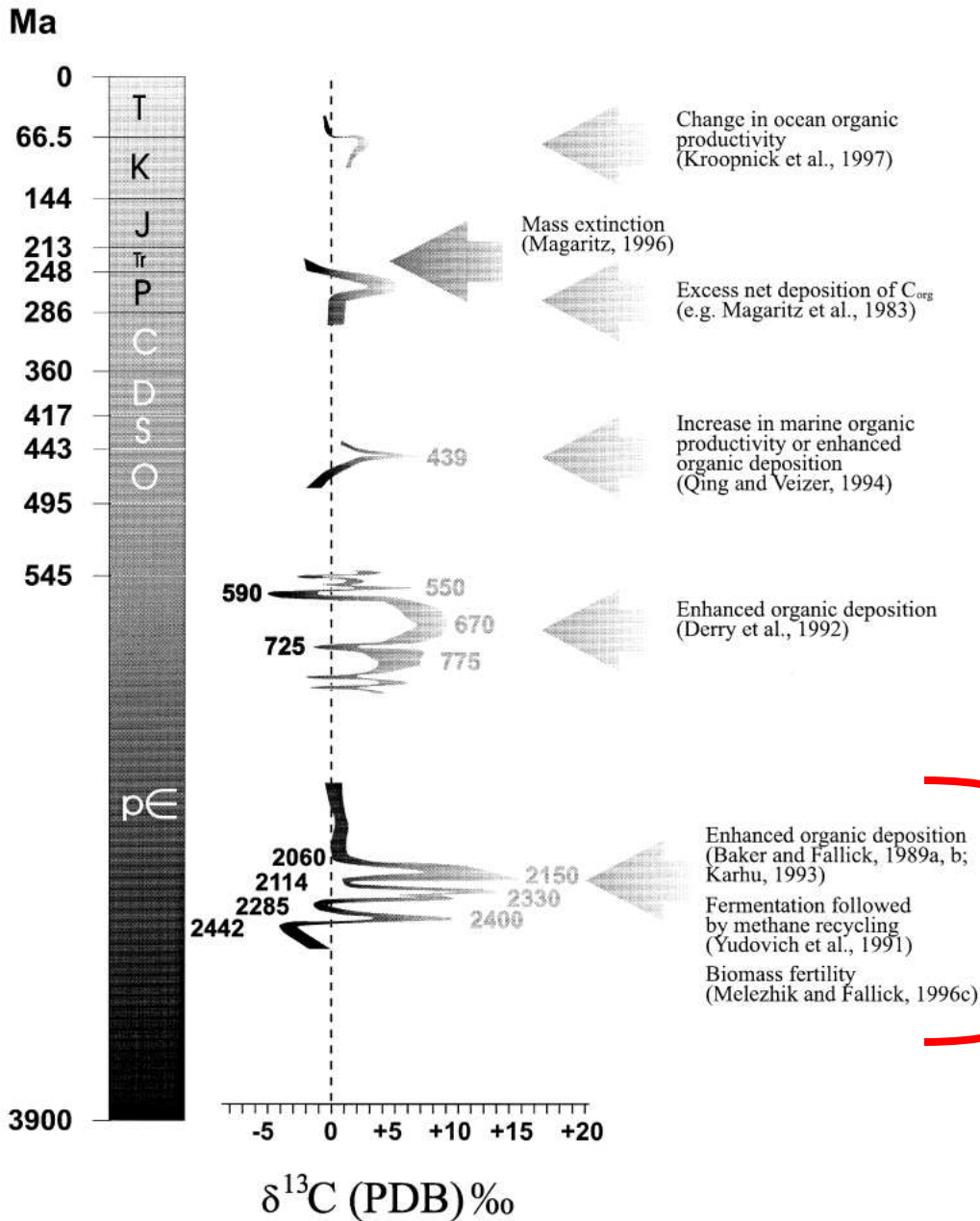
†References: 1-Babinski et al., 1995, 2-Barton et al., 1994, 3-Bowring et al., 1984, 4-Bros et al., 1992, 5-Chandler and Parrish, 1989, 6-Corfu and Andrews, 1986, 7-Gauthier-Lafaye and Weber, 1989, 8-Hassler, 1993, 9-Jahn and Cuvelier, 1994, 10-Jahn and Simonson, 1995, 11-Jahn et al., 1990, 12-Karhu, 1993, 13-Krogh et al., 1984, 14-Machado et al., 1992, 15-Machado et al., 1993, 16-Needham et al., 1988, 17-Page et al., 1994, 18-Page, 1988, 19-Pidgeon and Horwitz, 1991, 20-Russell et al., 1994, 21-Stern et al., 1993, 22-Strauss et al., 1992, 23-Treloar, 1988, 24-Trendall et al., 1990, 25-Veizer et al., 1990, 26-Veizer et al., 1992a, 27-Veizer et al., 1992b, 28-Walraven et al., 1990, 29-Welin, 1987.

§Two new analyses ($\delta^{13}\text{C} = 7.22\text{‰}$, 6.11‰) from the same location have been included.

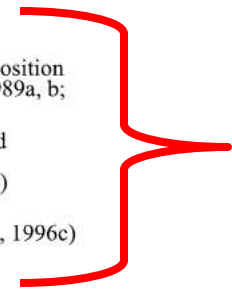
Karhu & Holland
1996

Figure 1. Variation in isotopic composition of carbon in sedimentary carbonates and organic matter during Paleoproterozoic time. Sources of isotopic and age data are given in Table 1. Mean $\delta^{13}\text{C}$ values of carbonates from Fennoscandian Shield from Karhu (1993) are indicated by open circles; data for all other carbonate units listed in Table 1 are indicated by closed circles. Vertical bars represent ± 1 standard deviation of $\delta^{13}\text{C}$ values, and horizontal bars indicate uncertainty in age of each stratigraphic unit. Arrows combine dated formations that are either preceded or followed by major $\delta^{13}\text{C}$ shift. BIF denotes field for iron and manganese formations. Note that uncertainties given for ages do not necessarily cover uncertainties in entire depositional periods of sample groups. PDB—Peedee belemnite.





Melezhik et al. 1999



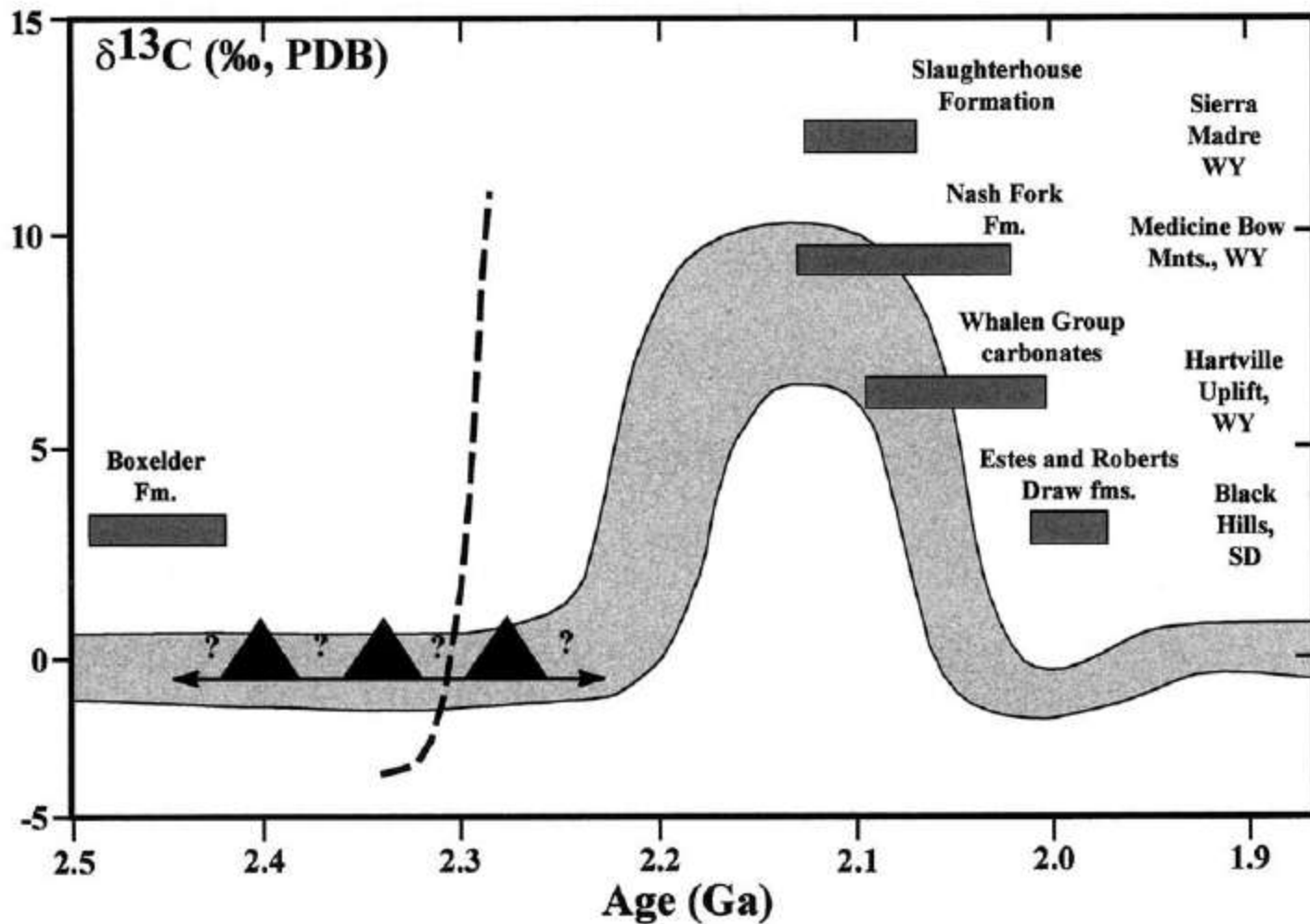


Fig. 10. Schematic representation of Paleoproterozoic secular carbon isotope variations after [Karhu and Holland \(1996\)](#) with additional information from [Bekker et al. \(2001a\)](#) shown by dashed line. Black triangles and question marks between them represent three Paleoproterozoic glacial events in North America and their age uncertainties. Studied units are arranged along the horizontal axis according to their geochronologic, lithostratigraphic, and chemostratigraphic age constraints (see text for discussion).

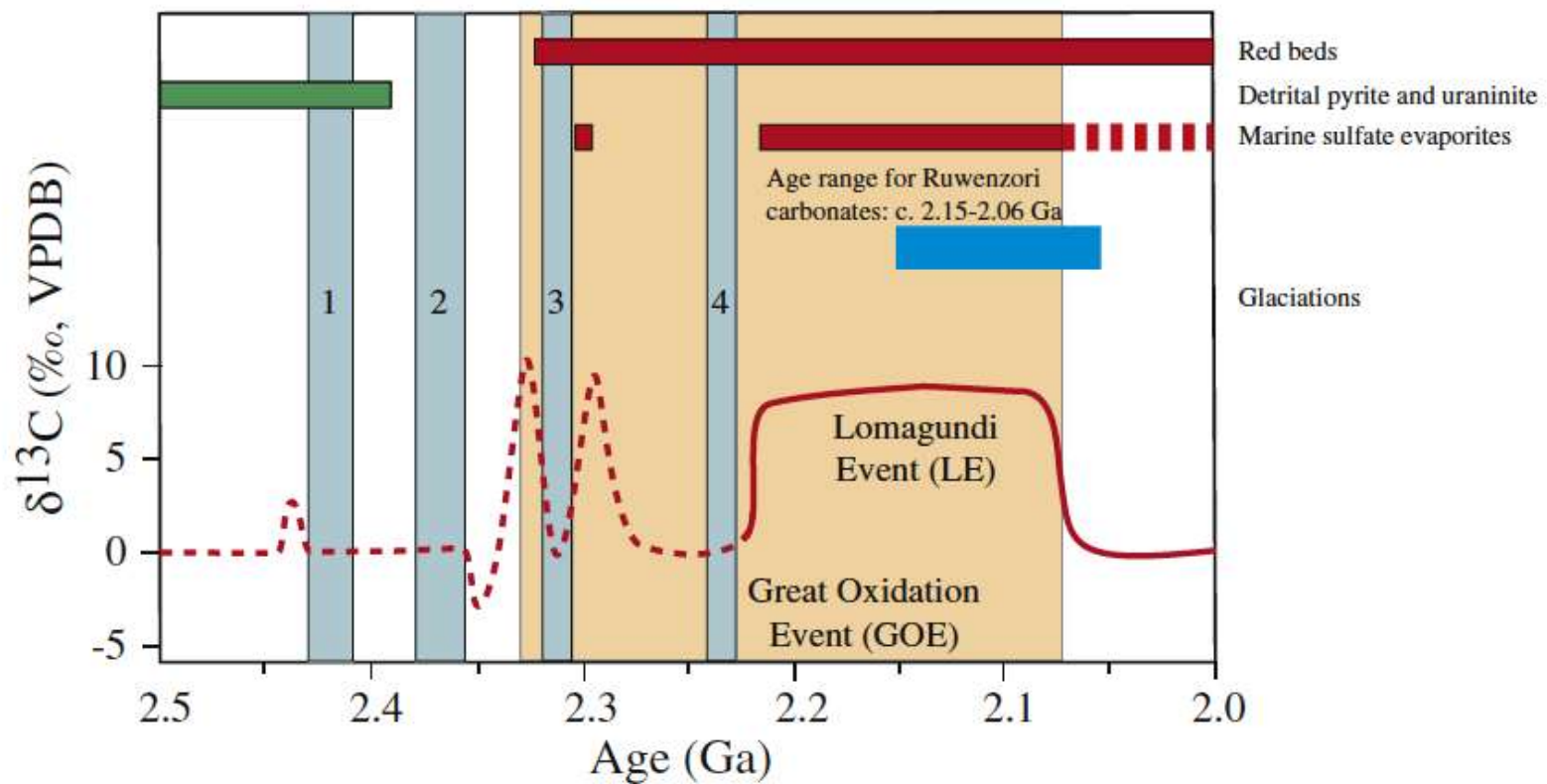
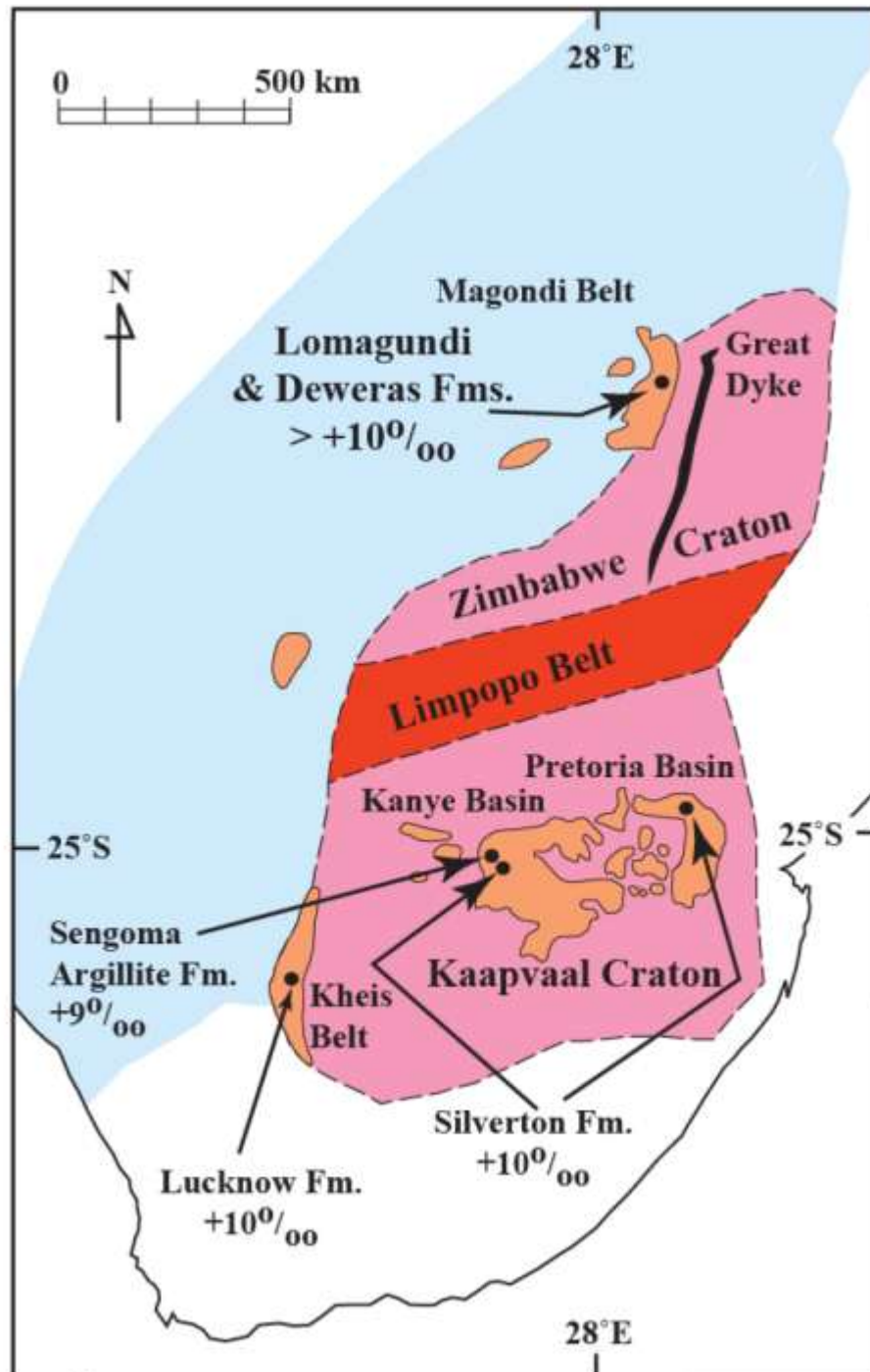


Fig. 4. Plot of $\delta^{13}\text{C}_{\text{carb}}$ values in ‰ VPDB vs. age (in Ma) for Paleoproterozoic sedimentary carbonates (after Bekker and Holland, 2012) showing data age range for Ruwenzori carbonates. Relevant redox indicators for the oxidation state of the atmosphere–ocean system and four blue vertical lines marking Paleoproterozoic glacial events are also shown (modified from Bekker and Holland, 2012). The dashed secular carbon isotope curve between 2.5 and 2.22 Ga emphasizes the uncertainty in this part of the curve, and the dashed bar for marine sulfate evaporites after c. 2.07–06 Ga indicates that sulfate evaporites again became scarce in the Paleoproterozoic and Mesoproterozoic records after that time.

Use of high $\delta^{13}\text{C}$
carbonate rocks in
chronostratigraphic
correlation

3. How the Magondi Belt lost its length



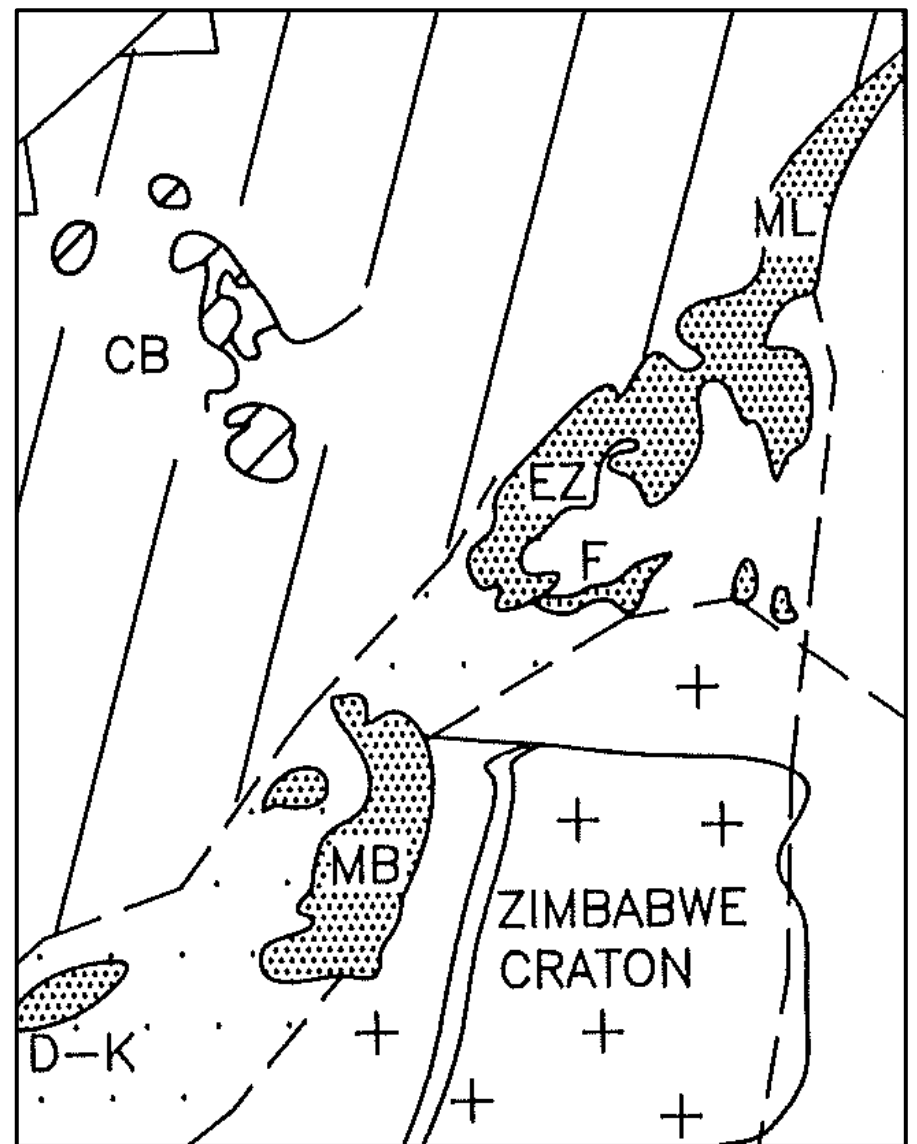
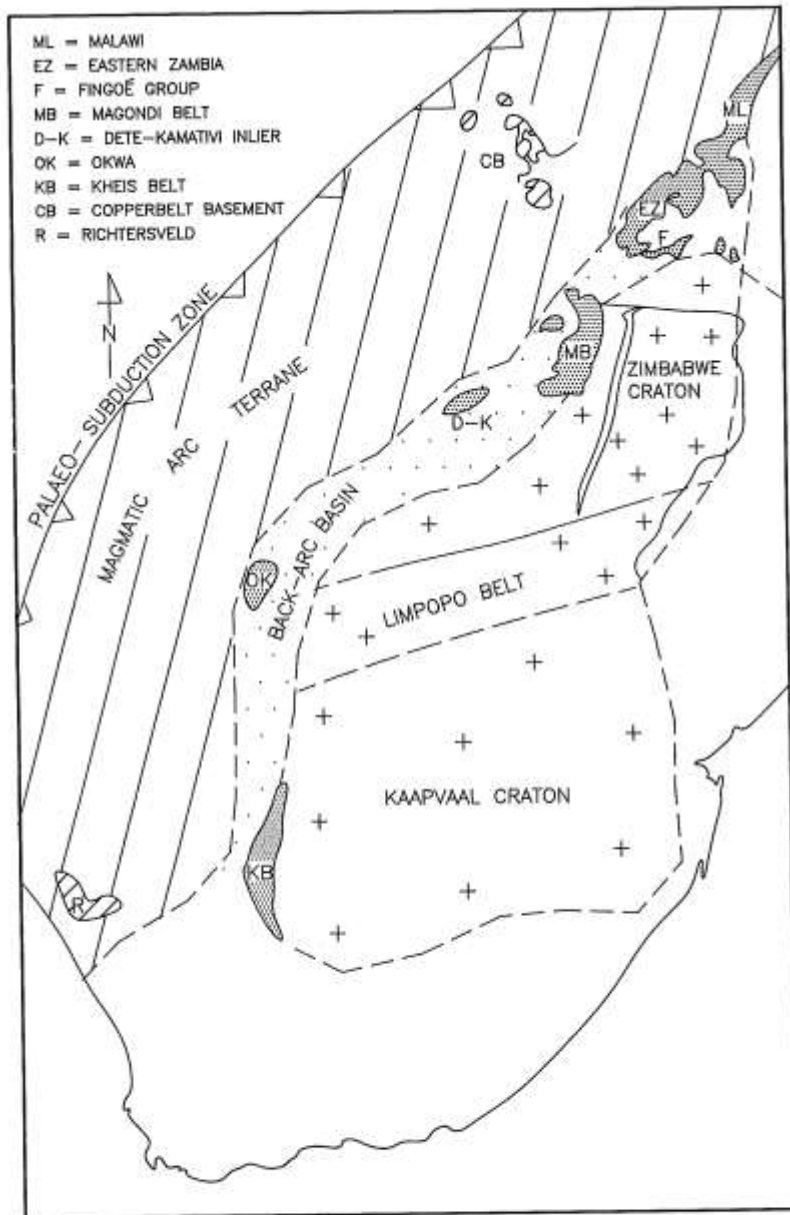


Figure 9: Schematic plan showing position of Magondi Supergroup and correlative sequences in a continental back-arc basin, with respect to the postulated magmatic arc terrane, palaeo-subduction zone, and the combined Zimbabwe-Limpopo-Kaapvaal continent (after Master, 1990d, 1991).

Master (1991a,b, 1994)

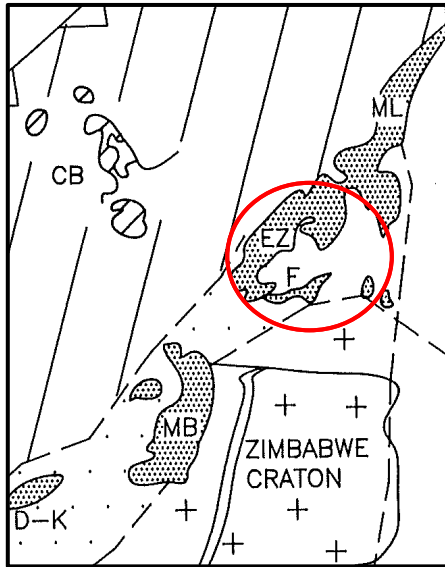
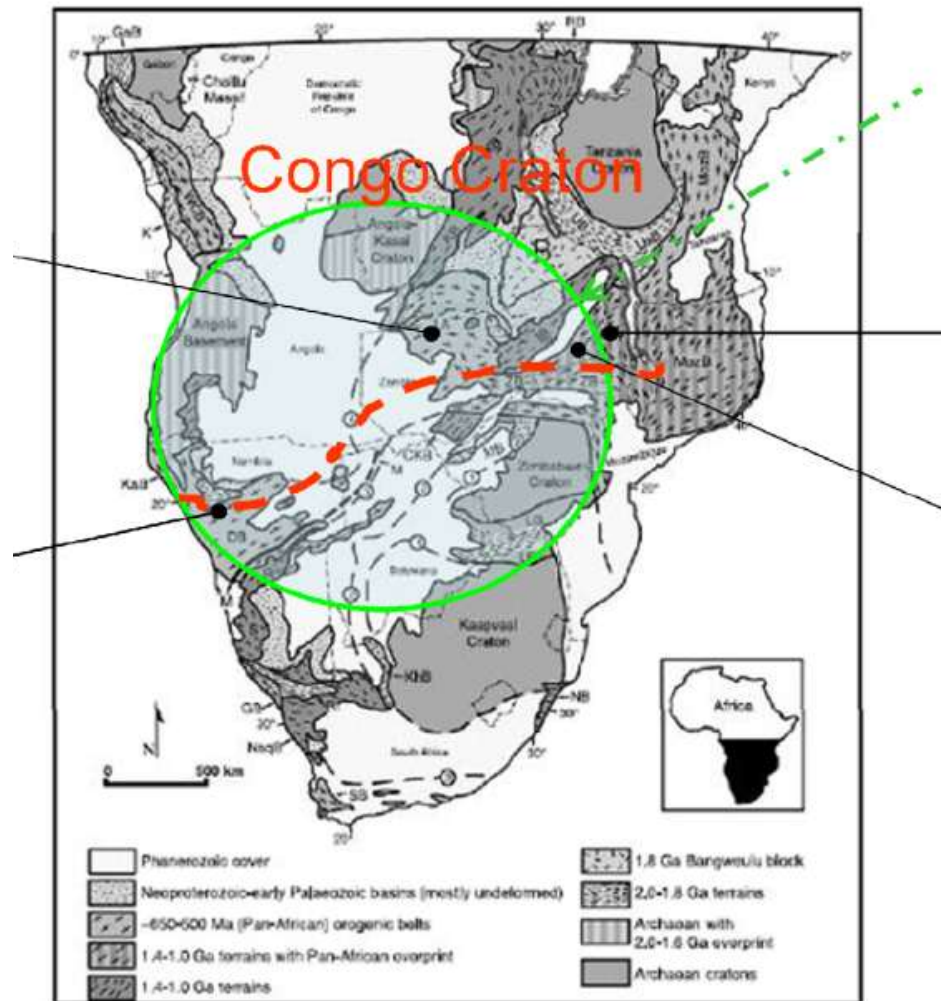


Table 1: Carbon and oxygen isotope geochemistry of marbles from the Mvuvye and Sinda

	$\delta^{13}\text{C}$ ‰V-PDB	$\delta^{18}\text{O}$ ‰V-PDB
Mvuvye Gp		
V-2	0.30	- 8.80
MV-3	-0.28	-10.53
MV-5	0.47	- 9.27
Sinda Gp		
CD-1	-1.30	-12.50
CD-3	-1.30	-12.70
CD-4	1.21	-12.31

Rifting on the southern margin of the Congo Craton, c. 765-730 Ma



Carbonate rocks in E Zambia (Mvuvye & Chindeni marbles):

$\delta^{13}C = -1.3$ to $+1.21$ ‰ VPDB

Therefore these marbles do NOT correlate with Magondi Belt

Southern Irumide Belt, Zambezi Belt and Zimbabwe Craton

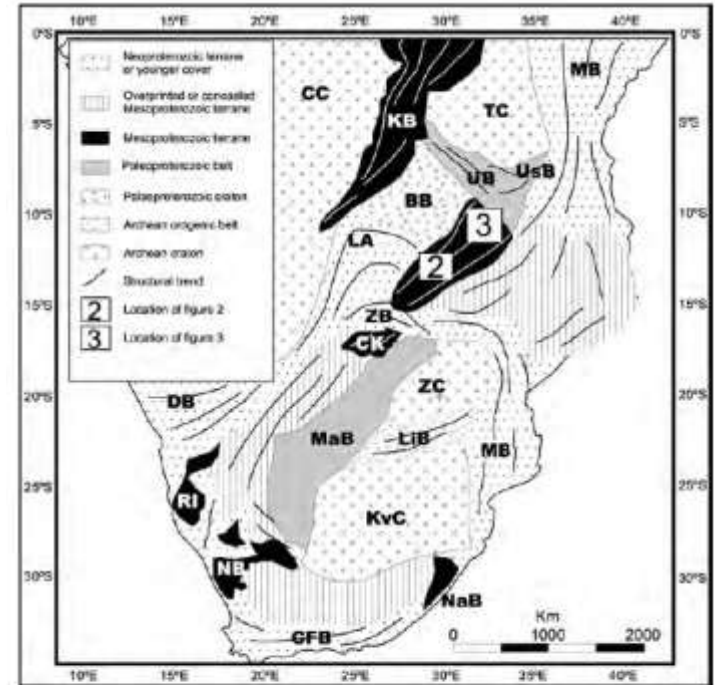
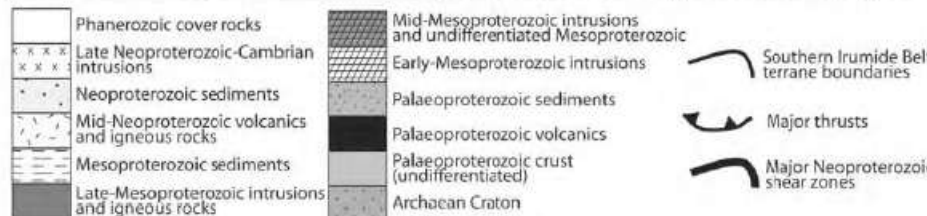
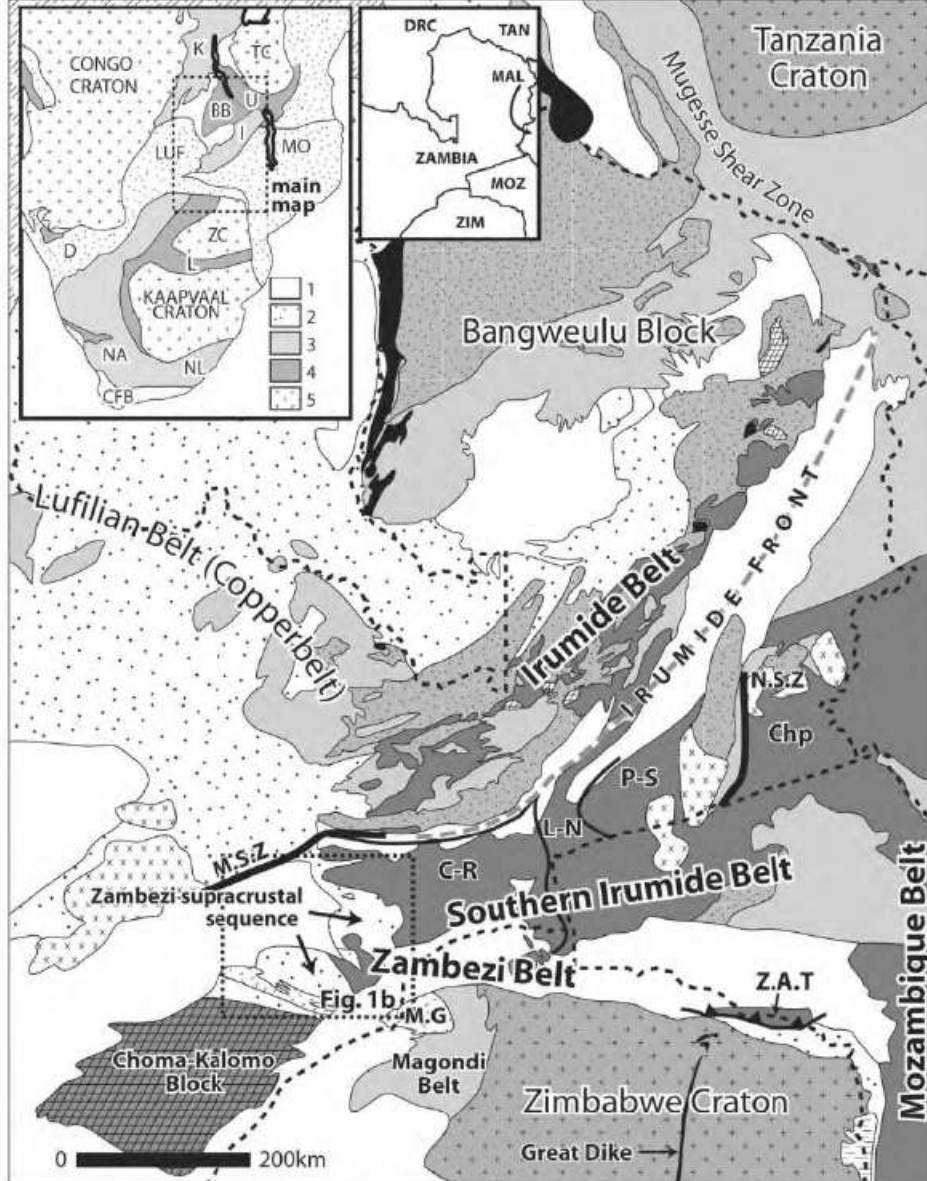


Figure 1. Tectonic provinces of central and southern Africa. Abbreviations: BB—Bangweulu block; CC—Congo craton; CFB—Cape fold belt; CK—Choma-Kalomo block; DB—Damara belt; KB—Kibaran belt; KvC—Kaapvaal craton; LA—Lufilian Arc; LiB—Limpopo belt; MaB—Magondi belt; MB—Mozambique belt; NaB—Natal belt; NB—Namaqua belt; RI—Rehoboth Inlier; TC—Tanzania craton; UB—Ubendian belt; UsB—Usagaran belt; ZB—Zambezi belt; ZC—Zimbabwe craton.

De Waele et al., 2003, Geology

Johnson et al. (2007). Journal of Geology, 115, 355-374.

Zambezi Belt- a suture zone during Gondwana amalgamation

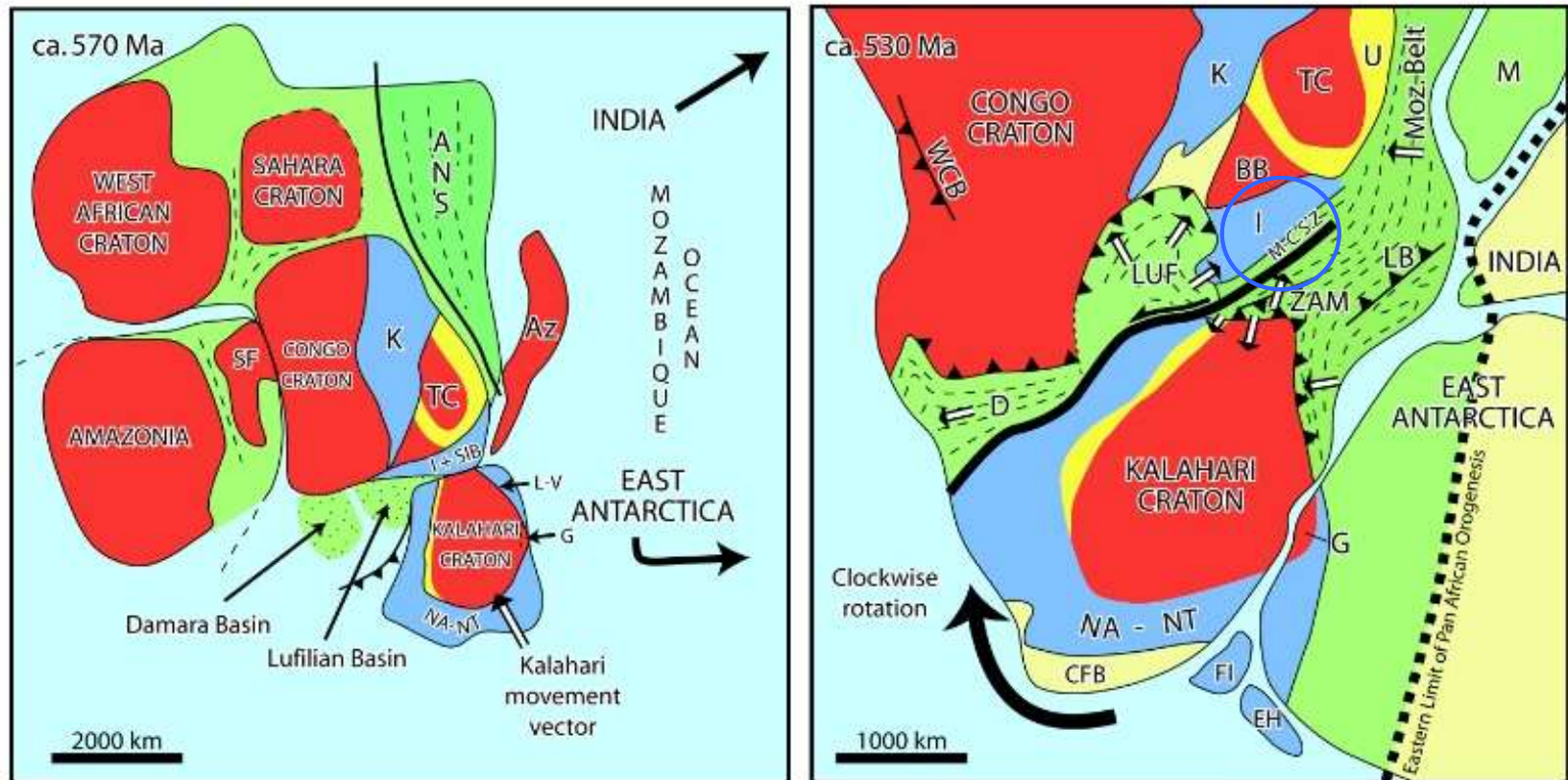


Figure 5. Cartoon showing the tectonic evolution and assembly history of the southern African cratons at a) 570 Ma and b) 530 Ma. Abbreviations as previous except: Az–Azania; EH–Ellsworth-Haag; FI–Falkland Islands; G–Grunehogna; LB–Lurio Belt; L-V–Lurio-Vijayan Peninsula; M-C SZ–Mwembeshi-Chimaliro Shear Zone; SF–Sao Francisco; SIB–Southern Irumide Belt; WCB–West Congo Belt.

Conclusions

- Carbon isotope analyses of marbles from the Petauke and Nyimba districts of Eastern Zambia (Sinda, Lusandwa and Mvuvye Groups) do not show the enrichments in $\delta^{13}\text{C}$ which are characteristic of the Magondi Supergroup carbonate rocks.
- The Magondi Belt did not extend further north than the Zambezi valley escarpment- it is separated from Eastern Zambia (“Southern Irumide Belt”) by a Neoproterozoic (“Pan-African”) suture

Acknowledgments

Funding from *University of the Witwatersrand;*
NRF-CIMERA

Support from UNESCO/IUGS *International*
Geological Correlation Program 363
for field work in 1996

